Eur. J. Mineral., 35, 1031–1049, 2023
https://doi.org/10.5194/ejm-35-1031-2023

European Journal of Mineralogy
Open Access

H_2O and Cl in deep crustal melts: the message of melt inclusions in metamorphic rocks

Silvio Ferrero[1], Alessia Borghini[2,3], Laurent Remusat[4], Gautier Nicoli[5], Bernd Wunder[6], and Roberto Braga[7]

[1]Dipartimento di Scienze Chimiche e Geologiche, Università degli Studi di Cagliari, Cittadella Universitaria di Monserrato S.S. 554 Bivio Sestu, 09042 Monserrato, Italy
[2]Faculty of Geology, Geophysics and Environmental Protection, AGH University of Science and Technology, 30-059 Kraków, Poland
[3]Institute of Geosciences, University of Potsdam, 14476 Potsdam, Germany
[4]Institut de Minéralogie, Physique des Matériaux et Cosmochimie, CNRS UMR 7590, Sorbonne Université, Muséum National d'Histoire Naturelle, CP52, 57 rue Cuvier, 75005 Paris, France
[5]Yorkshire Peat Partnership, BD23 1UD, Skipton, United Kingdom
[6]Helmholtz-Zentrum Potsdam, GFZ, 14473 Potsdam, Germany
[7]Dipartimento di Scienze Biologiche, Geologiche e Ambientali, Università di Bologna, Piazza di Porta S. Donato 1, 40126 Bologna, Italy

Correspondence: Silvio Ferrero (silvio.ferrero@unica.it)

Received: 22 July 2023 – Revised: 30 September 2023 – Accepted: 11 October 2023 – Published: 23 November 2023

Abstract. The use of NanoSIMS on primary melt inclusions in partially melted rocks is a powerful approach to clarify the budget of volatiles at depth during crust formation and its reworking. Anatectic melt inclusions are indeed gateways to quantify H_2O, halogens and other species (e.g. CO_2, N) partitioned into the deep partial melts generated during metamorphism of the continental crust. Here we present new datasets of NanoSIMS measurements of H_2O and Cl in preserved melt inclusions from metamorphic rocks with different protoliths – magmatic or sedimentary – which underwent partial melting at different pressure–temperature–fluid conditions. These new datasets are then compared with similar data on natural anatectic melts available in the literature to date. Our study provides novel, precise constraints for the H_2O content in natural melts formed at high pressure, a field previously investigated mostly via experiments. We also show that H_2O heterogeneities in partial melts at the microscale are common, regardless of the rock protolith. Correlations between H_2O contents and P–T values can be identified merging new and old data on anatectic inclusions via NanoSIMS. Overall, the data acquired so far indicate that silicate melt generation in nature always requires H_2O, even for the hottest melts found so far ($> 1000\,°C$). Moreover, in agreement with previous work, preserved glassy inclusions always appear to be poorer in H_2O than crystallized ones, regardless of their chemical system and/or P–T conditions of formation. Finally, this study reports the very first NanoSIMS data on Cl (often in amounts > 1000 ppm) acquired in situ on natural anatectic melts, showing how anatectic melt inclusions – additionally to magmatic ones – may become a powerful tool to clarify the role of halogens in many geological processes, not only in crustal evolution but also in ore deposit formation.

Published by Copernicus Publications on behalf of the European mineralogical societies DMG, SEM, SIMP & SFMC.

1 Introduction

Every inclusion hosted in a mineral is "a window into the rocks' past" (Ferrero and Angel, 2018). When properly interrogated, these inclusions yield a wealth of data on nature, genesis and evolution of the host-inclusion system and thus can be used to clarify how geological processes operate in shaping our planet (Esposito, 2021; Bartoli, 2021; Rose-Koga et al., 2021; Esposito et al., 2023; Borghini et al., 2023a). Deep fluids and melts are the most mobile, elusive and easily modified players in geological processes (Yardley, 2009; Connolly, 2010), yet their detailed characterization is fundamental to understand planetary evolution. Fluid and melt inclusions (FIs and MIs respectively) in metamorphic rocks offer direct access to these deep fluids – or better – to their manifestation stable at surface conditions, i.e. crystallized MI instead of melt (e.g. Ferrero et al., 2019, and references therein), and multiphase systems often composed of liquid + vapour ± crystal phases (e.g. Frezzotti and Ferrando, 2015; Carvalho et al., 2020). In the present work we define MI as inclusions which at the moment of entrapment/formation contained mostly a homogenous silicate melt, whereas FI trapped mostly volatile species, e.g. H_2O and CO_2, along with other minor volatile species (CH_4, N_2, Cl, F).

Often only few (tens of) micrometres across, these minute objects are thus gateways to the Earth's depths. The use of MI as tools to understand nature phenomena has a long-standing and time-honoured tradition, with the first publications on the topic dating back to second half of the 19th century (Sorby, 1858). During the 20th century they were then extensively employed in petrological studies of magmatic and volcanic system as well as ore deposits (Roedder, 1984; Lowenstern, 1995; Sobolev, 1996; Metrich and Wallace, 2008). The discovery of anatectic MI in granulitic enclaves (Cesare et al., 1997) at the closing of the last century, followed by their finding in regionally metamorphosed migmatites from different localities (Cesare et al., 2009; Ferrero et al., 2012), often crystallized as nanogranitoids (Bartoli et al., 2016), heralded the beginning of a new field of study, i.e. MI in metamorphic rocks (Cesare et al., 2015). In brief, they represent snapshots of the partial melt produced at depth and then encased (and preserved) in phases either generated or re-crystallized during melt production. From *lusus naturae* (freak of nature) found and investigated only in one location worldwide in 2009 (Cesare et al., 2009), the following decade saw the nanogranitoids becoming a well-established tool for metamorphic petrologists to constrain melt-producing reactions at depth (see Bartoli, 2021, and Nicoli and Ferrero, 2021, for the most up-to-date review), as well as to investigate how P–T–X conditions and fluids control anatectic melt composition (Acosta-Vigil et al., 2010, 2012, 2017; Bartoli and Carvalho, 2021; Nicoli et al., 2022a). These inclusions, whether they contain melt resulting from partial melting of the rock itself (Cesare et al., 1997; Acosta-Vigil et al., 2007; Cesare et al., 2015) or of nearby rocks and then trapped in re-crystallizing garnet, i.e. as metasomatizing melt (Borghini et al., 2018, 2020, 2023a), are the topic of the present work.

An aspect of utmost interest in deep melts studies is the identification and quantification of volatile elements (i.e. H, C, N, Cl, F). CO_2 in anatectic MI has been the topic of a recent string of publications (Nicoli and Ferrero, 2021; Nicoli et al., 2022a; Borghini et al., 2023a; Carvalho et al., 2023a); in this contribution we address exclusively H_2O and Cl. H_2O availability, either resulting from the breakdown of OH phase or present as infiltrating fluid, is crucial to stabilize a silicate melt at crustal conditions, and indeed the role of H_2O in crustal reworking and generations of granites is a matter of ongoing debate (Weinberg and Hasalová, 2015; Clemens et al., 2020). Moreover, the knowledge of the H_2O budget at depth is necessary to quantify melting as well as the melt behaviour on extraction, i.e. viscosity and density contrasts (e.g. Wickham, 1987; Brown, 2007; Nicoli et al., 2017; Nicoli, 2020). Cl and other halogens (e.g. fluorine) play a role both in shaping the partial melting reactions, e.g. by delaying melting toward higher T (Aranovich et al., 2013; Ferrero et al., 2021), and influencing the solubility of elements of economic interest and ore deposit formation (LaMadrid and Steele-McInnis, 2021). Working on anatectic MI offers the chance to measure directly in situ volatile species of interest and retrieve their original amounts, unadulterated and still preserved due to the lack of MI-matrix diffusion gradients commonly observed in magmatic MI (see discussion in Bartoli et al., 2014; Barth and Planck, 2021).

The present contribution reports novel Nano Secondary Ion Mass Spectrometry (NanoSIMS) results collected on re-homogenized nanogranitoids and preserved glassy inclusions (i.e. found already in a glassy state in the host mineral) of granitoid composition from metamorphic rocks. The use of SIMS, i.e. ion probes with spatial resolution in the order of 20–25 µm, to investigate volatiles in MI from magmatic rocks has become rather widespread in the last 2 decades (Hauri, 2002; Humphreys et al., 2006; Esposito et al., 2014; Bali et al., 2018; Rose-Koga et al., 2020, 2021). However, often magmatic MIs are found to be larger than anatectic ones, 100–50 µm (e.g. Roedder, 1979) versus 10–20 µm respectively; thus the latter require the use of a NanoSIMS rather than a normal SIMS. NanoSIMS (NS) investigation of preserved anatectic MI is a relatively novel approach – just like the concept of anatectic MI itself – and the analytical protocol was elaborated by Bartoli et al. (2014), the seminal work that jumpstarted the use of this technique on re-homogenized nanogranitoids. For our study we collected NS data on inclusions from three different case studies. The first case study is represented by nanogranitoids formed at near-ultrahigh-pressure (UHP) conditions in the Orlica–Śnieżnik Dome (OSD samples) in the Polish Sudetes (Bohemian Massif; see Ferrero et al., 2015, 2016, 2019). The second case study involves glassy inclusions from low-pressure garnet xenocrysts found at the Galite Islands (Tunisia), 20 km offshore Cape

Serrat (GA samples; see Ferrero et al., 2014). The third case study instead involves glassy inclusions in high-pressure (HP) eclogites from the Rubinberg quarry (RUB samples) in the Granulitgebirge (Bohemian Massif; see Borghini et al., 2018, 2020). These data are then compared with the existing database of H_2O and, where available, Cl contents so far measured on anatectic MI. Such a database covers a wide range of the metamorphic pressure–temperature (P–T) space (Acosta-Vigil et al., 2016; Carvalho et al., 2018; Bartoli et al., 2019; Ferri et al., 2020; Gianola et al., 2021), including HP (Ferrero et al., 2021) and UHP, in the diamond stability field (Borghini et al., 2023a), at least for H_2O contents. Novel and previously published data are then interpreted with the aim of identifying trends and thus the factors controlling the partitioning of H_2O and Cl in deep melts.

2 Sample description

In this work new data on H_2O and Cl were acquired on anatectic melt preserved as primary MI containing a crustal melt generated at very different P–T conditions and ages, as well as by a variety of melt-producing reactions. The protolith involved in the melting reaction is igneous in nature for the OSD and GA samples and a metasediment for RUB samples, as described in detail below.

The OSD samples are metagranitoids characterized by a leucocratic matrix of Qtz + Pl + Kfs with scattered porphyroblasts of nanogranitoid-bearing peritectic garnets (Fig. 1a) rich in Alm and Grs components (Alm_{58} Grs_{31} Pyr_{11} Sps_1), ternary feldspar, and limited kyanite formed at the metamorphic peak (Ferrero et al., 2015). The nanogranitoids have a constant phase assemblage of kumdykolite and kokchetavite (polymorphs of $NaAlSi_3O_8$ and $KAlSi_3O_8$ respectively), cristobalite or quartz (or more rarely tridymite), a residual glass, and calcite as a minor component (Ferrero et al., 2016). Such an assemblage is consistent with the crystallization of a hydrous granitic melt as confirmed by electron microprobe (EMP) results on re-homogenized inclusions (Ferrero et al., 2015, 2019; see also Wannhoff et al., 2022). Furthermore, both the successful re-homogenization of the nanogranitoids and classic geothermobarometers constrain partial melting near or at the metamorphic peak at $\sim 875\,^{\circ}C$ and 2.7 GPa, almost at UHP conditions, during the Variscan orogeny (Ferrero et al., 2015). Trace element data on the inclusions suggest the involvement of biotite in the melt production, thus pointing toward a delayed OH-phase dehydration melting (Ferrero et al., 2019). In these samples the bulk volatile content of the melt has been measured via NS exclusively on re-homogenized nanogranitoids as preserved glassy inclusions were not found in the investigated samples (e.g. Fig. 1b).

The GA samples were investigated in detail by Ferrero et al. (2014). The targeted garnets are metamorphic xenocrysts found in granodiorites intruding a flysch sequence (Belayouni et al., 2010). The host garnet has an Alm-rich core (Alm_{76} Pyr_{14} Grs_6 Sps_4) characterized by a large cluster of enclosed material that makes the core very dark (Fig. 1c). These clusters contain primary MI, FI and mixed (fluid + silicate melt) inclusions along with biotite, quartz, ilmenite, plagioclase and subhedral aggregates of white mica/sericite and chlorite interpreted as former cordierite (Ferrero et al., 2014). The MI range from fully crystallized to fully glassy, although the fully glassy inclusions are relatively rare and generally significantly smaller in size with respect to the crystallized ones (for inclusion petrography see Ferrero et al., 2014). When crystallized they contain quartz, K-feldspar/kokchetavite, biotite and albite/kumdykolite (Ferrero and Angel, 2018). Fluid inclusions contain a $CO_2 + H_2O + N_2 + CH_4$ fluid, always associated with small crystals of kaolinite and siderite, likely the result of fluid–host interaction (see also Carvalho et al., 2020). The mixed inclusions show variable proportions of glass and COHN fluid, e.g. from 30 %–70 % to 80 %–20 % based on visual inspection of the inclusions in thin section. Such microstructural features constrain garnet growth in the presence of a silicate melt and a COHN fluid under conditions of primary fluid–melt immiscibility (see e.g. Cesare et al., 2007). P–T calculation suggests that garnet formed at $\sim 800\,^{\circ}C$ and 0.35–0.5 GPa as a peritectic phase during fluid-present partial melting during the Miocene (Ferrero et al., 2014). NS analyses were performed exclusively on preserved glassy and mixed inclusions where the glassy portion was large enough, i.e. $> 4\,\mu m$ (e.g. Fig. 1d). No re-homogenization experiments were performed on these samples.

The RUB samples originate from an eclogite lens embedded in serpentinized garnet peridotites. The rock is dominated by garnet (Alm_{35} Prp_{39} Grs_{25} Sps_1) and clinopyroxene and was studied in detail by Borghini et al. (2018, 2020). Garnet contains tens of melt inclusions of 2–20 µm in diameter randomly distributed in wide clusters (Fig. 1e). Here, both nanogranitoids and glassy inclusions are present, although the latter are relatively smaller (2–5 µm) and rare, e.g. $< 10\,\%$ of the total (Fig. 1f). Nanogranitoids consist of kumdykolite or albite, phlogopite/biotite, osumilite, kokchetavite and carbonate (possibly calcite) and a variable amount of quartz, pyroxene and rare white mica (Borghini et al., 2018, 2020). Re-homogenization experiments were not performed on RUB samples, and the composition of the melt, including also Cl, was measured directly on the glassy inclusions via EMP. On the same glassy inclusions NS was used to quantify H_2O. The melt is granitic, peraluminous and rich in incompatible elements pointing toward the involvement of white mica in the melt producing reaction. Differently from the other two localities, here the melt is not trapped in its source rock. Geochemical and microstructural constraints show that it was produced via partial melting of metasediments belonging to subducted continental crust and then trapped in mantle-related bodies, i.e. the eclogitic bodies now visible on the field (Borghini et al., 2020). Previous studies have estimated the metamorphic peak at 1000–1015 °C and

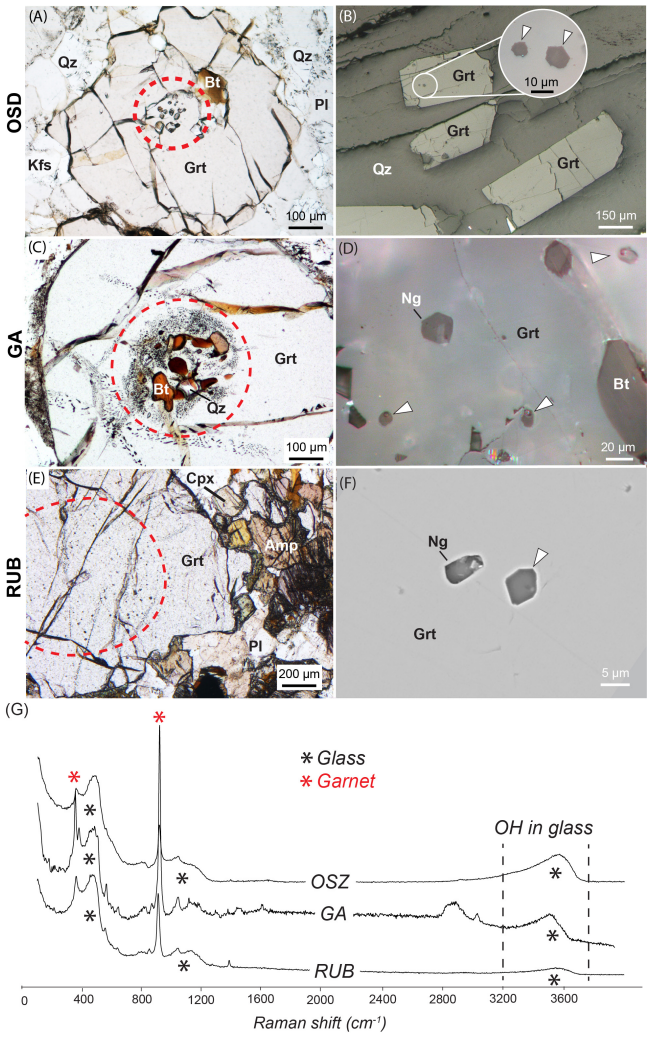

Figure 1. Features of the targeted samples. Panels **(a)**, **(c)** and **(e)** show the petrographic features of the MI-bearing garnets and **(b)**, **(d)** and **(f)** the features of their inclusions. Microraman spectra acquired on glassy inclusions (after re-homogenization for OSD and in natural samples for GA and RUB) from the three different case studies are reported in **(g)**. The large band at $\sim 2800\,cm^{-1}$ in GA spectrum is due to the presence of araldite in the analysed volume. Ng – nanogranitoids; white arrows – glassy inclusions with or without bubbles and mixed inclusions in the sole case of GA samples (in **d**). Mineral abbreviations after Whitney and Evans (2010). For sample abbreviations see text.

2.0–2.2 GPa during the Early Carboniferous (340 Ma; Rötzler et al., 2008; Hagen et al., 2008).

3 Methods

In our study we used a piston cylinder press, a NanoSIMS, an electron microprobe and microraman spectroscopy. The use of the piston cylinder was necessary to re-melt the nanogranitoids entirely in OSD samples beforehand, to obtain a homogenous glass suitable for NS and EMP analyses. We used a Johannes-type piston–cylinder apparatus operated at GeoForschungsZentrum (GFZ) Potsdam (Germany). Garnet chips with unexposed nanogranitoids were manually separated under microscope observation from doubly polished thick sections and used as starting material in experiments. Four or five chips per each experiment were loaded in platinum capsules of 4 mm length and 3 mm diameter and cold-sealed after filling. Powdered silica was added in the capsule both as a pressure medium and to isolate the chips from each other and from the capsule walls. No water was added to the experimental charge. The pressure cells consisted of talc–pyrex glass outer sleeves with graphite furnace and crushable alumina inner spacers in which the Pt capsule was embedded (see methods in Bartoli et al., 2013a; Cesare et al., 2015; Ferrero et al., 2015). The T in the capsule was controlled using a Type S thermocouple (Pt–PtRh10) with a $\pm 10\,°C$ uncertainty. The assemblage has been pressure calibrated via the equilibrium quartz = coesite according to Mirwald and Massonne (1980), which is accurate within 50 MPa. The assemblage was then kept in the press at 875 °C and 2.7 GPa for ~ 24 h and resulted into the complete re-homogenization of the large majority of the nanogranitoids (more details in Ferrero et al., 2019). Quenching of the experimental charges took place at high P, and the machine was unloaded only after reaching ambient T. The capsules were then mounted in epoxy and polished to expose re-homogenized inclusions. As each garnet chip generally contains only < 10 re-homogenized inclusions after repolishing, we performed 5 experimental runs at these conditions to re-homogenize enough material to obtain a significant dataset.

Microraman spectroscopy was performed to verify glassy nature and homogeneity of the re-melted nanogranitoids before NS analyses. We used a HORIBA Jobin Yvon LabRAM HR 800 at the Institute of Geoscience, University of Potsdam. An air-cooled Nd:YAG laser was used for excitation ($\lambda = 532$ nm, laser power on the sample of 2–3 mW) with a grating of 300 lines mm^{-1}, slit width and confocal hole set to 100 and 200 µm, respectively. The Raman spectra of re-homogenized glass inclusions were acquired with a 100× objective in the wavenumber range 100–4000 cm^{-1}, integrating three repetitions of 30 s with spectral resolution of 10 cm^{-1}.

Both GA and RUB samples contain glassy inclusions ready to be analysed by NS means. Glassy inclusions of suitable size, i.e. > 4 µm in size, were identified via optical investigation of doubly polished thick sections, and the host garnets manually separated to form multiple garnet chips. The glassy nature of the selected inclusions was also verified via microraman spectroscopy before proceeding with NS analyses (Fig. 1g).

In situ NS analyses were performed to quantify H_2O and Cl during two analytical sessions in May 2016 and January 2017 for samples OSZ and GA and in February 2020 for RUB samples using the CAMECA NanoSIMS 50 oper-

ated at the Muséum National d'Histoire Naturelle of Paris, following the approach of Bartoli et al. (2014) and Créon et al. (2018). Polished capsules with re-homogenized inclusions (OSD samples), garnet chips with glassy inclusions (GA samples) and portions of thin sections with garnets containing glassy inclusions (RUB samples) were mounted in indium along with standard glasses. The inclusions were then identified through images of $^{28}Si^-$ and $^{56}Fe^{16}O^-$ secondary ions. Each analysis was preceded by pre-sputtering on a $5 \times 5\,\mu m^2$ surface area for 2 min to remove gold coating, to minimize surface contamination and to achieve a steady-state sputtering regime (Thomen et al., 2014). Data acquisition was performed with a 20 pA Cs+ primary beam by rasterization of a $3 \times 3\,\mu m^2$ surface area. Ions were exclusively collected from the inner $1 \times 1\,\mu m^2$ using the beam blanking mode, to minimize surface contamination. Each analysis consisted of 200 cycles with a duration of 1.024 s. Secondary ions of $^{16}OH^-$ (proxy for H_2O), $^{28}Si^-$, $^{35}Cl^-$ and $^{56}Fe^{16}O^-$ were recorded simultaneously in multicollection mode, using electron multipliers with a dead time of 44 ns. Mass resolution was set to 5500 to resolve mass interference on these ions. Only analyses with a stable $^{16}OH^-/^{28}Si^-$ and $^{35}Cl^-/^{28}Si^-$ ratios were considered in this study. Three glasses of leucogranitic composition and known concentrations of H_2O, varying between ~ 0.3 wt, % and 4.86 wt, %, were used for calibration (Bartoli et al., 2014; see also Supplement). For Cl concentration, we used NIST 610 and 612 standards (at 273 and 88 ppm, respectively) in addition to an anhydrous leucogranitic glass DL (Morgan and London, 2005) being Cl free to determine $[Cl]/[SiO_2]$ ratios from $^{35}Cl^-/^{28}Si^-$. Analytical uncertainty on each NS measurement was based on the Poisson error due to counting statistics and was combined with the uncertainty on the calibration (corresponding to 68 % interval of confidence in the regression line) by quadratic sum to obtain the uncertainty at 68 % on values reported in Table 1 for the different analytical sessions. Cl in RUB glassy inclusions was measured by EMP means using acceleration voltage 15 kV, current 3.5 nA and beam diameter 1 µm. The detection limit for Cl during these analyses has been estimated to be 0.011 wt % or 110 ppm.

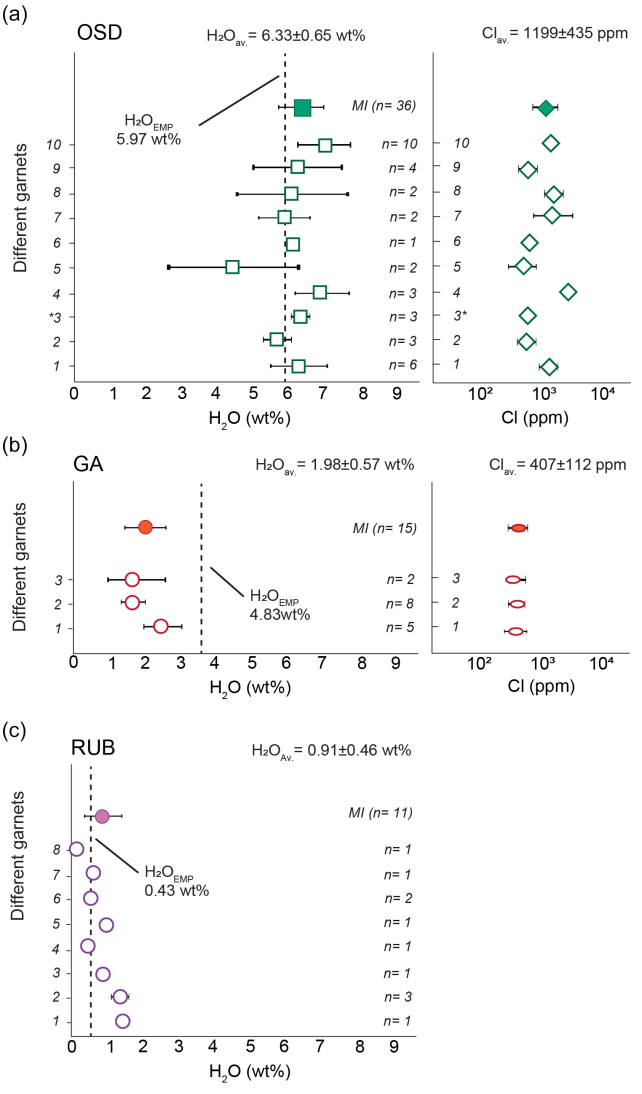

Figure 2. NanoSIMS results on H_2O and Cl contents in the anatectic melt inclusions from OSD, GA and RUB samples. $*$ denotes glass in interstitial pocket. Dashed lines – difference of the average EMP totals from 100 for each case study. H_2O_{EMP} – average H_2O contents from EMP difference (H_2O_{EMP}) are from Ferrero et al. (2019) for OSD, Ferrero et al. (2014) for GA and from the Supplement of Borghini et al. (2018) for RUB.

4 Results

A grand total of 47 analyses were acquired in the OSD granulites on 35 re-homogenized inclusions from 8 different garnets – few inclusions were large enough to allow for multiple analyses as visible in Table 1. Some inclusions only contained glass resulting from nanogranitoid re-homogenization, whereas others contain quartz (see column "comment" in table 1). The latter is interpreted to be a phase trapped during inclusion formation (hence not precipitated from the enclosed melt), as previous studies did not identify any compositional difference between glassy and glassy inclusions with quartz (Ferrero et al., 2019). Three further analyses were acquired on a glass pocket at the contact between the quartz matrix enveloping the garnet chips and the chip itself. The measured H_2O contents in the re-homogenized nanogranitoids range from 3.07 wt % to 8.33 wt %, with an average of 6.33 wt %. When different garnet crystals are considered, the H_2O content varies from 4.38 wt % to 6.97 wt % on average (Fig. 2a). The measured Cl content ranges from ~ 350 to ~ 2800 ppm, with an average of ~ 1200 ppm. H_2O and Cl contents show a weak positive correlation (Fig. 3). The measured glass pocket shows an average H_2O content of 6.33 wt %, identical to the overall EMP average of the

Table 1. H_2O and Cl in the three investigated case studies. Analyses acquired on the same inclusions are indicated with the same letter. In comments we report the features of each investigated inclusion at the moment of NS analytical session – see text for clarifications.

Case study	Grt	MI	Point	Comment	H_2O (wt %)	1σ error	Cl (ppm)	1σ error	Case study	Grt	MI	Point	Comment	H_2O (wt %)	1σ error	Cl (ppm)	1σ error
OSD	1	*a*	OSZ-7_1	glass + Qz	7.32	0.11	1319	24			*h*	OSZ-11_10	glass	6.91	0.11	1455	27
		a	OSZ-7_2		6.99	0.11	1263	23			*i*	OSZ11_1	glass + Qz	8.50	0.19	1619	9
		a	OSZ-7_3		7.11	0.11	1183	22			*i*	OSZ11_2		8.37	0.19	1364	8
		b	OSZ-7_4	glass + Qz	4.75	0.10	646	13			*i*	OSZ11_3		6.79	0.18	1196	7
		c	OSZ7_2	glass + Qz	6.67	0.18	1477	8			*l*	OSZ11_4	glass + Qz	7.11	0.18	1193	7
		c	OSZ7_3		6.26	0.18	1553	9			*m*	OSZ11_5	glass + Qz	8.58	0.19	1691	9
		d	OSZ7_5	glass	6.46	0.18	1514	8			*m*	OSZ11_6		8.09	0.19	1440	8
		e	OSZ7_6	glass	6.75	0.18	1399	8			*n*	OSZ11_8	glass + Qz	7.52	0.18	1471	8
		f	OSZ7_7	glass	6.26	0.18	1350	8									
									GA	1	*a*	Gal1_1	glass	3.15	0.10	444	10
	2	*a*	OSZ-7_5	glass + Qz	5.77	0.10	445	10			*b*	Gal1_2	glass + bubble	2.46	0.10	362	9
		a	OSZ-7_6		6.06	0.10	473	10			*c*	Gal1_3	glass	1.96	0.10	214	8
		b	OSZ-7_7	glass	5.89	0.10	452	10			*d*	Gal1_4	glass + bubble	1.96	0.10	614	12
		c	OSZ7_1	glass	5.20	0.17	785	5			*e*	Gal1_5	glass + bubble	2.85	0.10	400	9
	3**	*a*	OSZ7_8	interstitial	6.46	0.18	608	4		2	*a*	Gal2_1	glass + bubble	1.50	0.10	432	9
		b	OSZ7_9	interstitial	6.10	0.17	585	4			*b*	Gal2_2	glass + bubble	1.65	0.10	304	8
		c	OSZ7_10	interstitial	6.42	0.18	598	4			*c*	Gal2_3	glass + bubble	1.86	0.10	352	9
											d	Gal2_4	glass + bubble	1.32	0.10	242	8
	4	*a*	OSZ8_1	glass	7.76	0.18	2788	16									
		b	OSZ8_2	glass	6.54	0.18	2515	14		3	*a*	Gal2_8	glass + bubble	1.44	0.10	544	11
		c	OSZ8_3	glass	6.38	0.18	2457	14			*b*	Gal2_9	glass + bubble	1.74	0.10	400	9
											c	Gal2_10	glass + bubble	1.67	0.10	316	8
	5	*a*	OSZ10_1	glass	3.07	0.17	357	3									
		b	OSZ10_2	glass	5.53	0.17	696	4		4	*a*	Gal2_11	glass + bubble	2.46	0.10	258	8
		b	OSZ10_3	glass	5.85	0.17	700	4									
										5	*a*	Gal4_1	glass + bubble	2.38	0.10	302	8
	6	*a*	OSZ10_4	glass + Qz	6.42	0.18	690	4			*b*	Gal4_2	glass + bubble	1.22	0.10	282	8
		a	OSZ10_5		5.85	0.17	620	4									
		a	OSZ10_6		5.97	0.17	626	4									
									RUB	1	*a*	CS5Grt5cG_1	glass	1.45	0.08	*0.11	na
	7	*a*	OSZ-8_1	glass	5.32	0.10	1038	19									
		b	OSZ-8_2	glass + Qz	6.38	0.10	2409	44		2	*a*	CS5Grt5dG_2	glass	1.54	0.07	*0.11	na
											b	CS5Grt5dG_3	glass	1.37	0.08	*0.09	na
	8	*a*	OSZ-9_1	glass	4.92	0.10	1315	24			*c*	CS5Grt5dG_4	glass	1.22	0.08	*0.12	na
		b	OSZ-9_2	glass	7.48	0.11	2242	41									
		b	OSZ-9_3		6.99	0.11	2074	38		3	*a*	CS9Grt1G_1	glass	0.92	0.08	*0.08	na
		b	OSZ-9_4		6.99	0.11	2037	37									
										4	*a*	CS17Grt1G_1	glass	0.54	0.09	*0.06	na
	9	*a*	OSZ10_1	glass + Qz	4.67	0.10	417	10									
		b	OSZ10_4	glass	5.81	0.10	600	12		5	*a*	S1Grt1G_1	glass	1.04	0.08	*0.05	na
		c	OSZ10_2	glass + Qz	7.28	0.11	751	14									
		d	OSZ10_3	glass + Qz	7.15	0.11	732	14		6	*a*	S5Grt5aG_1	glass	0.61	0.09	*0.04	na
											b	S5Grt5aG_3	glass	0.53	0.09	*0.08	na
	10	*a*	OSZ-11_3	glass	6.50	0.10	1200	22									
		b	OSZ-11_4	glass + Qz	6.30	0.10	1155	21		7	*a*	S5Grt5eG_1	glass	0.66	0.09	*0.08	na
		c	OSZ-11_5	glass + Qz	6.30	0.10	1122	21									
		c	OSZ-11_6		6.22	0.10	1123	21		8	*a*	S9Grt1G_1	glass	0.09	0.10	*0.05	na
		d	OSZ-11_7	glass + Qz	6.30	0.10	1272	23									
		e	OSZ-11_8	glass + Qz	6.50	0.10	1312	24									
		e	OSZ-11_9		6.63	0.10	1375	25									

* Chlorine (in wt %) estimated via EMPA on the same inclusions. ** Glass in interstitial position. na – not analyzed.

dataset, whereas the average Cl content (600 ppm) is roughly half of the overall EMP average. One single inclusion (corresponding to analysis OSZ10_1) shows significantly lower H_2O and Cl with respect to the other analyses, suggesting that the inclusion underwent volatile loss.

In the GA samples we analysed 15 inclusions from 3 different garnets. The size of the inclusions was generally $< 10\,\mu m$ in diameter and did not allow for multiple analyses; moreover, the analysable surface of the glassy inclusion is furthermore reduced by the common occurrences of bubbles (Fig. 1d). The measured H_2O content of the glassy inclusions ranges from 1.22 wt % to 3.15 wt % with an average of 1.98 wt %. When the different garnets are considered, the average H_2O content ranges from 1.62 wt % to 2.48 wt %. The measured Cl content ranges between ~ 200 and ~ 600 ppm, with an average of ~ 370 ppm, without a clear correlation with H_2O (Fig. 2).

For the RUB samples, NS data were collected on 11 inclusions from 9 garnets. As in the previous case study, the small size of the inclusions ($\leq 10\,\mu m$) did not allow for multiple analyses. The H_2O contents range from 0.09 wt % to 1.54 wt %, with an average of 0.91 wt %. The Cl contents re-

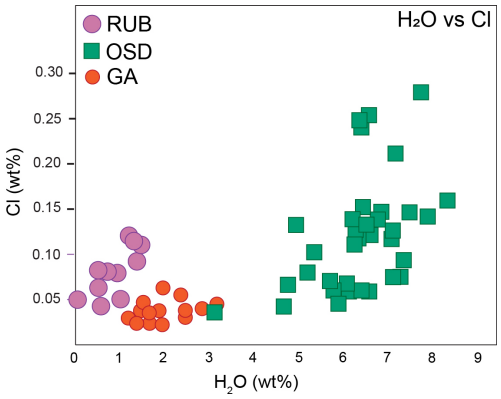

Figure 3. H_2O versus Cl content in anatectic MI. Cl was measured via NS in OSD and GA (this study; see Fig. 2), and via EMP in RUB (Table 1 in this study).

ported in Table 1 and in Fig. 3 were measured via EMP on the same inclusions and then analysed via NS, and they show a positive correlation with the H_2O content.

5 Discussion

5.1 Reliability of anatectic MI for volatile quantification

Volatiles in deep melts are a crucial piece of the puzzle represented by deep natural processes of crustal reworking. It is thus self-evident how important it is to extract reliable information from MI in metamorphic rocks. However, are these inclusions reliable probes of the volatile content of deep melts? The first NS work on nanogranitoid from the Ronda migmatites from Bartoli et al. (2014) already tackled the problem of their reliability in terms of H_2O quantification in a comprehensive way, providing an overwhelmingly positive answer to this question. This complemented the work of Bartoli et al. (2013a), where similar conclusions were reached using EMP and microraman data. This conclusion has then received further, unequivocal support and strength from the wealth of nanogranitoid studies over the last decade (Ferrero et al., 2019; Nicoli and Ferrero, 2021; Bartoli, 2021). For sake of brevity, here we discuss only what we think are the two strongest pieces of evidence: the lack of chemical/pressure gradients and their successful re-homogenization by experimental means.

Magmatic MIs forming in olivine sitting in a crystallizing magma experience important pressure and chemical gradients because they are surrounded by a degassing magma in a melt-dominated system (discussion in Bartoli et al., 2014). Conversely, an anatectic MI forms in a solid-dominated system, e.g. a rock, which is slowly undergoing partial melting with generation of small amounts of melt, at least in the initial stages. If partial melting proceeds, the system may achieve melt connectivity (likely at 7 vol % of melt; Rosenberg and Handy, 2005), thus leading to the melt being rapidly drained and preventing its accumulation in the source rock. The lack of a chemical or pressure gradient due to the absence of large batches of magma in the rock at any given time thus prevents the anatectic MI from losing (as well as gaining) H_2O after entrapment – obviously this is true only when evidence of decrepitation, such as cracks, is absent in the inclusions (see also Bartoli et al., 2014).

Experimental re-homogenization (Bartoli et al., 2013a, b) is a fundamental step in nanogranitoid studies. Experimental reheating under confining P is performed using a piston cylinder press, without adding water. This leads to the re-homogenization of formerly polycrystalline inclusions into melt, and then, after quenching to glass, it allows direct analyses via EMP and other in situ techniques. The P–T conditions chosen for the experimental runs correspond to the host formation, and they are obtained beforehand via independent methods (thermodynamic modelling, classic geothermobarometers). Admittedly, in the majority of case studies (see e.g. Ferrero et al., 2019, 2021; Gianola et al., 2021, to name a recent few), multiple experiments at variable P–T conditions were necessary to obtain complete re-homogenization. Such a discrepancy may be the combined result of garnet growth, and thus melt entrapment, occurring before the rock attains (and record) metamorphic peak conditions, as well as intrinsic error/uncertainties of the different approaches used for P–T estimation. However, this experimental approach eventually proved successful, i.e. led to complete re-homogenization, in every single nanogranitoid investigation performed so far (Nicoli and Ferrero, 2021, for the most up-to-date list, Ferrero et al., 2021; Borghini et al., 2023a; see also Liu et al., 2023). The re-homogenization of formerly crystallized nanogranitoids at T substantially consistent with that calculated via other approaches is in itself clear evidence that H_2O is not lost after entrapment. H_2O loss would in fact shift the melting T of the enclosed melt to higher T, as proven by the extensive literature on haplogranitic melts, or altogether prevent the re-homogenization in case of complete H_2O loss (Makhluf et al., 2017, and references therein; Ferrero et al., 2019).

In a nutshell, every single piece of evidence so far collected on the topic of H_2O content modifications in nanogranitoids strongly supports the fact that they preserve their original H_2O content. The reliability of Cl – as well as of other halogen – measurements in anatectic MI has not been investigated so far (see also Sect. 5.5 below). However, previous studies on MI in both natural systems and experiments show that the fates of H_2O and Cl in melts are coupled (Webster et al., 2018), making it therefore likely for the Cl content of anatectic MI to be representative of the original one. All of these considerations thus allow us to confidently delve deeper into what these in situ measurements of volatiles in melts tell us about deep processes of crustal reworking.

5.2 Novel NS data on H_2O in silicate melts

Two out of the three new case studies addressed in the present contribution, i.e. OSD and RUB samples, preserve crustal melts generated at HP conditions, i.e. in the range 1.6–3.0 GPa, consistent with deep continental subduction. Our study reports novel NS data on volatiles from these two case studies, marking a significant advancement in terms of knowledge of natural granitoid melts in HP rocks. So far, natural HP melts have been investigated in the partially melted metasediments of the Central Maine Terrane (CMT) in terms of geochemical composition – including volatiles (Ferrero et al., 2021) – whereas previous studies on the OSD (Ferrero et al., 2015, 2019) and RUB samples (Borghini et al., 2018, 2020) investigated here did not target the volatiles.

NS measurements on the OSD samples show that the HP silicate melt trapped at 875 °C (Ferrero et al., 2015) contains ∼ 6 wt % of H_2O (average, $n = 36$). The silicate melt in RUB samples is much less hydrous, with an average of ∼ 1 wt % ($n = 11$) consistently with a significantly higher entrapment T (1000–1050 °C; Borghini et al., 2018). The work so far performed on nanogranitoids suggests that they can be regarded as "ideal natural experimental charges of melt" (Ferrero et al., 2015), making the existent corpus of knowledge on experimental melts the most straightforward term of comparison to better understand the message of these inclusions. Caution is however advised insofar significant discrepancies are to be expected. For instance, experiments may not be fully representative of natural processes due to metastability phenomena, as discussed in detail by Bartoli (2021). Moreover, Carvalho et al. (2023a) have recently pointed out how NS data on natural MI show often higher H_2O contents with respect to those observed in experimental melts produced at similar P–T–fluid conditions, likely due to differences in oxygen fugacity. Despite these caveats, when we compare our novel results with the H_2O isopleths of a melt of granitic composition from experiments, we can observe some striking correspondence. In particular, the OSD melt has H_2O contents remarkably consistent with the results of Hermann and Spandler (2008) at 2.7 GPa (Fig. 4). Similarly, previously published data for the CMT samples of Ferrero et al. (2021) show that the average H_2O content of 4.4 wt % measured in the melt is consistent with the (extrapolated) experimental results on haplogranitic melts in the field 1000–1050 °C and 1.7–2.0 GPa (Fig. 4).

Such remarkable similarity between nature and experiments on (simplified) granitic melts does not however hold for the melt in the RUB samples, which are far less hydrous despite (1) having similar protolith and P–T formation conditions to the CMT nanogranitoids and (2) likely being the product of a fluid-assisted partial melting (Borghini et al., 2018, 2020). The most likely explanation lies in the geochemical features of the melt source, an hypothesis which cannot however be satisfactorily tested due to the absence of

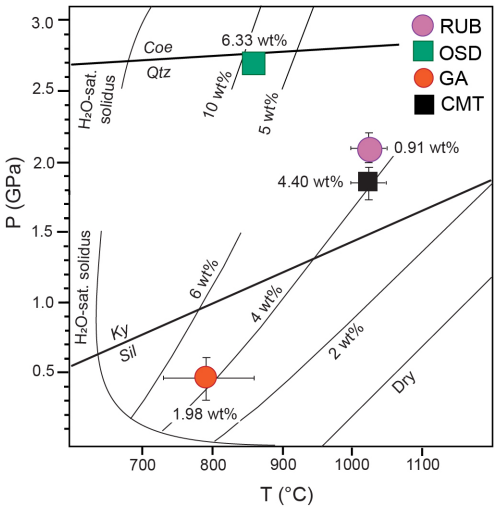

Figure 4. P–T diagram with comparison between NS data of HP anatectic MI versus experiments on granitic melts from literature. The H_2O isopleths of the melt at $P \leq 2.2$ GPa are from Makhluf et al. (2017) and references therein. For melts at $P \geq 2.5$ GPa we use curves from Hermann and Spandler (2008). The H_2O contents of the experimental melts come from mass balance calculations.

suitable metasedimentary lithologies in the surrounding of the sample location in the Granulitgebirge.

With respect to the previous case studies, the melt hosted in the GA samples was instead trapped at much shallower, mid-crustal conditions, ∼ 0.5 GPa and ∼ 800 °C (Ferrero et al., 2014). Our NS measurements on GA glassy inclusions show an average H_2O content of ∼ 2 wt % with a maximum amount of 3.15 wt %. Interestingly, both values are significantly lower than the average fluid content estimated via difference from EMP totals, 4.2 wt % (after alkali-loss correction; see Ferrero et al., 2014). The latter value represents the total amount of volatile species dissolved in the preserved glass, thus suggesting that in this case study a significant aliquot of the fluids is likely represented by volatiles other than H_2O and Cl (∼ 400 ppm or 0.04 wt % average). In this particular case study the investigated MI occurs in clusters along with multiphase inclusions containing CO_2, N_2 and CH_4 visible under microraman investigation. This was interpreted as evidence for primary fluid–melt immiscibility, i.e. the garnet grew in presence of both a silicate melt and a COHN fluid (Ferrero et al., 2014). Thus, such constraints suggest that the melt in GA samples contain C as the main volatile other than H_2O, along with minor N. Primary fluid–melt immiscibility in peritectic garnets was first reported by Cesare et al. (2007) and then recognized over the following decade in 12 out of 50 case studies of nanogranitoids, i.e. 25 % of the total (Nicoli and Ferrero 2021), including in Archean samples from Greenland (Nicoli et al., 2022b). Such findings provide a very strong support to the idea that partial melting at depth takes often place in presence of a

COHN fluid rather than a simple H_2O-rich fluid (Carvalho et al., 2020, and references therein).

5.2.1 H_2O heterogeneities at the microscale

The NS dataset collected on the OSD samples is the largest to date on a single case study and consists of 45 analyses on 36 different nanogranitoids (Table 1), collected on 10 different garnets. The average H_2O contents of the inclusions clearly display a certain spread when grouped per garnet, from ~ 4.4 wt % in garnet 5 ($n = 2$) to ~ 7 wt % in garnet 10 ($n = 10$; Fig. 2), despite their occurrence in a fairly homogenous rock such as a metagranitoid.

Heterogeneities in H_2O contents of similar magnitude were already reported in the very first work about NS measurements on re-homogenized inclusions from the Ronda migmatites by Bartoli et al. (2014), where the average values reach almost a 200 % variation (5.4 wt % to 9.1 wt %). The authors proposed that such a feature may be the result of microscale-level compositional differences of the phase assemblage reacting to produce melt at relatively low T, ~ 700 °C, and 0.5 GPa (Bartoli et al., 2013b).

Droplets of melt are indeed likely trapped by the peritectic garnet as soon as the dehydration melting starts (Cesare et al., 2015), making it plausible for the initial melt forming in different locations (hence different batches) inside the same rock to have slightly different compositions. Such variability would also be more pronounced if the host rock underwent only a limited degree of melting, which would prevent the achievement of significant melt interconnectivity between different batches and, therefore, melt homogenization across the whole rock volume (Acosta-Vigil et al., 2017). Indeed, both Ronda migmatites and the OSD metagranitoids (this study) likely experienced limited melting, i.e. < 10 vol % (Bartoli et al., 2015) and 5 vol %–15 vol % (Roberts and Finger, 1997, on similar rocks) respectively, thus making it plausible that also the OSD MI contains an initial melt with variable H_2O content because of being buffered by (slightly) different phase assemblages; i.e. see the concept of mosaic equilibrium proposed by Bartoli et al. (2014).

A further factor likely to favour heterogeneities in H_2O activities in different melt pools is the presence of graphite – a common rock-forming mineral in metasediments such as the Ronda samples. However, graphite is notably absent in metaigneous rocks such as the OSD samples, and this may have helped the system to maintain a narrower H_2O content variability in these rocks vs. the Ronda metasediments.

5.3 Comparison with the existent database of H_2O NS data on re-homogenized anatectic MI

The NS approach has generated to date a rich database consisting of 236 single analyses on anatectic melts of broadly granitoid composition (Table 2). These analyses belong to 11 different datasets, each one corresponding to a nanogranitoid population trapped at specific P–T conditions. In some cases, multiple datasets are from the same work. Carvalho et al. (2018) investigated three nanogranitoid populations from rocks melted at different P–T conditions, e.g. the upper amphibolite facies, transition zone and granulite facies visible in Table 2 as C18-UA, C18-Tr and C18-G, respectively, all of them from the Ivrea–Verbano Zone. Acosta-Vigil et al. (2016) instead report two nanogranitoid populations, one in the garnet core (AV16a) and one in the garnet rim (AV16b), which record two separate melting events in the same garnet. Data from Borghini et al. (2023a) are treated as two datasets as one analysis comes from a re-homogenized inclusion (B23a), whereas the remnants are from preserved glassy inclusions (B23b). The complete set of case studies considered, their relevant features and related literature are visible in Table 2, while the raw data on NS analyses are reported in the Supplement (Table S1).

First of all, case studies where nanogranitoids occur with FI in the same cluster (white squares with blue rims in Fig. 5) do not show any significant difference in H_2O content with respect to those where only nanogranitoids are present (blue squares; see also related caption). Another very apparent feature emerging from the inspection of these diagrams is that the NS data from glassy inclusions of the two new case studies reported here, GA and RUB (circles in Fig. 5), are clearly far removed from the bulk of the data so far collected on re-homogenized nanogranitoids. They display significantly lower H_2O contents with respect to other melts at similar conditions (Fig. 5a) – this aspect will be discussed in detail in Sect. 5.4. As for the re-homogenized nanogranitoids, the average H_2O contents measured so far via NS range from 4.40 wt % of the HP metasediments of the Central Maine Terrane (Ferrero et al., 2021) to 10.31 wt % at mid-crustal pressure in Jubrique (Acosta-Vigil et al., 2016). Most of the analyses ($n = 145$, or 60 % of the total) have been so far performed on melt trapped at $P \leq 1.5$ GPa and $T \leq 900$ °C. The average H_2O contents display a negative correlation with T (Fig. 5b; see also Carvalho et al., 2023a), consistent with the available experimental data on H_2O in silicate melt, which predict that silicate melts are able to accommodate less H_2O as the T increases (Johannes and Holtz, 1996). Interestingly, the NS measurements available so far show H_2O contents higher than experimental melts at similar T, as recently pointed out by Carvalho et al. (2023a) and ascribed to differences in oxidizing conditions between natural, often graphite-bearing rocks and experiments.

Interestingly, a sizable amount of H_2O is commonly measured even in very hot melts, e.g. at $T > 1000$ °C, when they formed at HP and UHP conditions (this study; Ferrero et al., 2021; Borghini et al., 2023a). Decades of work on UHP melts/fluids (Hermann and Rubatto, 2014, and references therein) have shown how the minimum H_2O content of a melt increases with P at constant T; i.e. see the positive slope of the *liquidus* curves of experimental melts (Fig. 4). However, our compilation shows that the average H_2O content

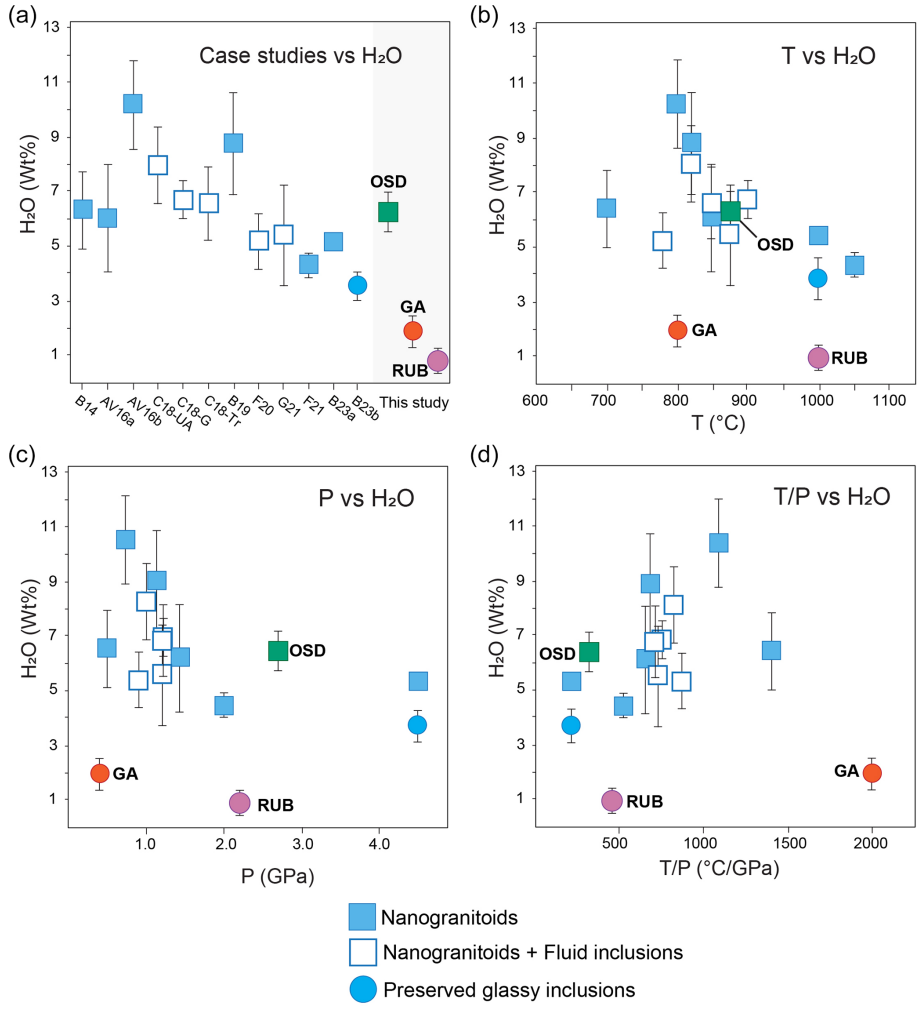

Figure 5. Comparison between this study and the literature. In the legend "Nanogranitoids" identifies case studies were only primary nanogranitoids were identified and "Nanogranitoids + FI" those in which the nanogranitoids occur along with syngenetic FI. For the latter group, the reported H_2O content corresponds exclusively to the one measured via NS in nanogranitoids. The data are reported as average analyses and standard deviations for each case study. The abbreviations used in **(a)** are explained in Table 2.

in nanogranitoids, regardless of the presence or absence of fluids, correlates negatively with pressure (Fig. 5c). Such a trend is likely to be a simple artifact, as in the investigated case studies P and T increase simultaneously during burial, making the observed decrease in H_2O content more likely to be driven by the co-increase of temperature. This is visible in Fig. 5d, where the thermobaric gradients display a positive correlation with H_2O contents.

Discrepancies between nature and experimental setups must also be considered. Progressive H_2O loss via dehydration reactions during burial before the attainment of suprasolidus conditions is likely to limit – more or less severely – the amount of H_2O available for melt production at depth (e.g. Connolly and Thompson, 1989), whereas experiments are generally run in presence of a H_2O-bearing fluid. In other words, the experiments give us insights into how much H_2O can be accommodated in deep melts if a H_2O-bearing fluid is present, but such a condition is clearly not always satisfied in nature. Finally, novel data on natural anatectic MI at HP and UHP conditions suggest that the solubility of other important volatiles such as C (see discussion in Borghini et al., 2023a) and possibly halogens (see below) in silicate melts increases with P, thus lowering the H_2O activity in the melt, but this needs to be supported by further in situ measurements of volatiles in natural deep melts. In conclusion, all of the factors mentioned above – synchronous T increase during burial, limited H_2O availability and increasing importance of other volatiles – are likely to concur in lowering the H_2O contents measured in natural partial melts as they are produced deeper and deeper in subducted continental crust.

No NS data are available on silicate melts produced at $T >$ 900 °C and low–medium P, i.e. in the ultra-high-temperature (UHT) field (Kelsey and Hand, 2015). Experimental evidence on the stability of granitic melts calls for the possibility

Table 2. Datasets used in Fig. 4. The whole analytical database is reported in the Supplement. The P–T conditions of MI formation reported in the table correspond either to the experimental re-homogenization conditions or to the results of phase equilibria modelling on the host rock. SD = standard deviation 1σ.

Name	H_2O	SD	No. data	P (GPa)	T (°C)	T/P	Inclusion occurrence	Location	Melt source	Reference	Comment
B14	6.44	1.42	27	0.5	700	1400	MI	Ronda (Spain)	Metasediments	Bartoli et al. (2014)	–
AV16a	6.13	1.95	8	1.3	850	654	MI	Jubrique (Spain)	Metasediments	Acosta-Vigil et al. (2016)	Inclusion from garnet core
AV16b	10.31	1.63	15	0.7	800	1143	MI	Jubrique (Spain)	Metasediments	Acosta-Vigil et al. (2016)	Inclusion from garnet rim
C18-UA	8.08	1.40	6	1.0	820	820	MI + FI	Ivrea–Verbano Zone (Italy)	Metasediments	Carvalho et al. (2018)	Upper amphibolite facies
C18-Tr	6.67	1.33	22	1.2	850	708	MI + FI	Ivrea–Verbano Zone (Italy)	Metasediments	Carvalho et al. (2018)	Transition zone
C18-G	6.80	0.69	17	1.2	900	750	MI + FI	Ivrea–Verbano Zone (Italy)	Metasediments	Carvalho et al. (2018)	Granulite facies
B19	8.86	1.86	16	1.2	820	683	MI	Kali Gandaki (Himalaya)	Metasediments	Bartoli et al. (2019)	–
F20	5.27	1.03	17	0.9	780	867	MI + FI	Lanterman Range (Antarctica)	Metasediments	Ferri et al. (2020)	–
F21	4.40	0.46	12	2.0	1050	525	MI	Central Maine Terrane (US)	Metasediments	Ferrero et al. (2021)	–
G21	5.50	1.84	17	1.2	875	729	MI + FI	Gruf complex (Central Alps)	Metagranitoids	Gianola et al. (2021)	–
B23a	5.23	–	1	4.5	1000	222	MI	Erzgebirge (Germany)	Metasediments	Borghini et al. (2023a)	–
B23b	3.70	0.61	7	4.5	1000	222	MI	Erzgebirge (Germany)	Metasediments	Borghini et al. (2023a)	Preserved glassy inclusion
OSD	6.38	0.72	45	2.7	875	324	MI	Orlica–Śnieżnik Dome (Poland)	Metagranitoids	This study	–
GA	1.98	0.57	15	0.4	800	2000	MI + FI	Galite Islands (Tunisia)	Metagranitoids	This study	Preserved glassy inclusion
RUB	0.91	0.46	11	2.2	1000	455	MI	Rubinberg (Germany)	Metasediments	This study	Preserved glassy inclusion

of generating a completely anhydrous melt at T in excess of 1100 °C and $P < 0.2$ GPa (Johannes and Holtz, 1996). However, so far no natural case study of nanogranitoids has shown the existence of completely dry melt. Even the two cases of anatectic MI formed in the UHT field so far found in nature, i.e. from the Kerala Khondalite Belt in southern India (Cesare et al., 2009) and the Lützow–Holm Complex in East Antarctica (Carvalho et al., 2023b), still contain ~ 0.5 wt % H_2O (difference from EMP totals only; Ferrero et al., 2012) and < 1.3 wt % H_2O (difference from EMP totals and microraman investigation), respectively. Similarly, nanogranitoids in sapphirine – a typical UHT mineral – were reported by Gianola et al. (2021) to contain a muscovite-bearing phase assemblage, thus confirming again that even UHT minerals trap hydrous melts. Overall, NS data on anatectic MI agree with previous nanogranitoid works in supporting the message of the experiments, insofar as the generation of silicate melts during regional metamorphism and crustal subduction requires the presence of H_2O (e.g. Makhluf et al., 2017).

5.4 H_2O content in glassy versus crystallized inclusions

H_2O contents from re-homogenized nanogranitoids are clustered together, whereas data from glassy inclusions are at significantly lower H_2O values when our new NS data are plotted against nanogranitoid literature (Fig. 5). This may raise an important, fundamental question: does the re-homogenization procedure somehow change the H_2O content of the melt? Previous work (Bartoli et al., 2014) has shown that this is not likely, as the re-homogenization experiments are conducted without adding H_2O; i.e. all the H_2O required to re-melt the nanogranitoid assemblage must be already present in the crystallized inclusion. H_2O can be bound in the structure of the OH-bearing phases, as visible from microraman maps on the inclusions (Bartoli et al., 2013b; Ferrero et al., 2016, 2021) and/or interstitially as a free fluid (Bartoli et al., 2013b) and/or hosted in a residual glass (Ferrero et al., 2015, 2016). Thus, the large difference in H_2O content is likely to be an intrinsic feature of the inclusions.

Glassy inclusions were found in many nanogranitoid studies and proven via EMP analyses to contain a melt chemically identical, in terms of major and minor elements, to the one hosted in the coexisting nanogranitoids (Cesare et al., 2009; Bartoli et al., 2013b, 2016; Borghini et al., 2018; Gianola et al., 2021). This was expected based on microstructural constraints coming from fluid inclusion studies. For example, glassy and crystallized MI do coexist in the same cluster; they are primary and therefore they must have been trapped at the same time during host formation (Roedder, 1984). However, glass in natural rocks is commonly found in rapidly cooled magmatic rocks and thus represents an oddity in slowly cooled regionally metamorphosed rocks. When first reported by Cesare et al. (2009) for anatectic MI in migmatites of the Kerala Khondalite Belt (India), this occurrence was tentatively correlated to the fact that glassy inclu-

sions are statistically smaller than nanogranitoids present in the same cluster and the presence of glass ascribed to the inhibition of mineral nucleation due to the small size of the pore hosting the melt (Cesare et al., 2009). Advancements in nanogranitoid studies, fuelled by a continuously growing list of case studies across the world, have then clarified that a "size-based" explanation cannot hold. Glassy inclusions of diameter larger than that of nanogranitoids were indeed found coexisting in the very same cluster in Bartoli et al. (2015). This led the authors to propose instead that the H_2O content of the single inclusions is the most likely controlling factor in terms of melt crystallization vs. glass preservation over geological times. This problem was comprehensively tackled by Tacchetto et al. (2021) by comparing H_2O contents of glassy inclusions and re-homogenized nanogranitoids obtained via difference from EMP total, NS and calibrated microraman spectroscopy. The authors showed that glassy inclusions in metamorphic rocks are significantly less hydrous than re-homogenized nanogranitoids, 2.7 wt % vs. 6.9 wt % H_2O. Mean values are calculated respectively on 106 glassy inclusions and 505 re-homogenized nanogranitoids (Fig. 12 in Tacchetto et al., 2021) sharing an overall similar granitoid composition.

A variable H_2O content influences melt behaviour on crystallization in two main ways. First, from 3 wt % to 7 wt % the viscosity of a granitoid melt changes 2 orders of magnitude for a given T (Scaillet et al., 1996), thus leading to inhibition of the mineral nucleation process in more anhydrous melts. Secondly, higher H_2O contents lower the glass transition T; i.e. a more hydrous melt has more time to crystallize on cooling, thus leading to the formation of nanogranitoids rather than glassy inclusions (Tacchetto et al., 2021).

The most straightforward consequence of this finding is that investigating exclusively preserved glassy inclusions in natural metamorphic rocks will likely lead to the underestimation of the average H_2O content of the melt, as already pointed out by Tacchetto et al. (2021). A quantification of this underestimation was provided by Borghini et al. (2023a) working on MI from Saidenbach eclogites (Bohemian Massif). There, NS data on glassy inclusions display a mean H_2O content 25 % relatively lower than in a re-homogenized nanogranitoid containing the same melt. In the present work, NS data were collected exclusively on glassy inclusions from RUB samples. However, these results can be directly compared with the H_2O content on re-homogenized nanogranitoids from the nearby Klatschmühle HP eclogites (Borghini et al., 2018), estimated via difference from EMP totals. The latter MIs likely entrap the same granitic melt found in the RUB samples (Borghini et al., 2020) and contain ∼ 1.3 wt % H_2O average vs. 0.9 wt % in glassy inclusions from RUB samples, suggesting that the H_2O in glassy inclusions is likely underestimated of ∼ 40 % with respect to the average H_2O content in the melt. Further work based on NS analyses on glassy and crystallized inclusions from the same clusters

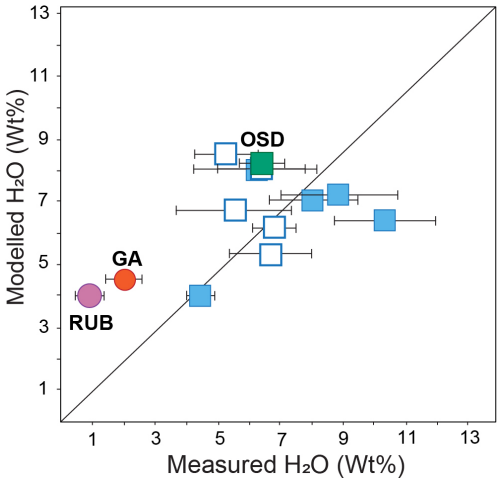

Figure 6. Modelled melt H_2O (wt %) vs. measured H_2O content in inclusion (wt %). Symbols: see Fig. 5. Plotted results are reported in Table S3 in the Supplement.

is clearly needed to firm up these values, which to date have been based on a rather small database.

We performed exploratory phase equilibria modelling on different protoliths to evaluate whether the models could reproduce the measured H_2O contents in glassy and re-homogenized inclusions. We chose appropriate starting compositions – average Phanerozoic shale, greywacke and granite from Condie (1993; reported in Table S2 in the Supplement) – depending on the protolith of each case study. The modelling was performed following the approach of Nicoli and Dyck (2018) using Perple_X version 6.9.0 (Connolly, 2010) in the system NCKFMASHT with the 2011-updated Holland and Powell (1998) dataset and the following a–x models: silicate melt, garnet, white mica, biotite, orthopyroxene, cordierite, chlorite (White et al., 2014); sapphirine (Holand and Powell, 1998), ilmenite–hematite (White et al., 2000); plagioclase and orthoclase (Holland and Powell, 2003); and amphibole (Diener and Powell, 2012). Bulk-rock water contents were individually fixed to produce saturated solidus conditions at the point where the prograde P–T path intersects the solidus, as defined by the thermobaric gradient associated with each dataset (Table 2). In some cases, melt inclusions coexisted with a COH-rich fluid-phase (datasets F20, C18a-b-c, G21, GA) or they were trapped during a partial melting reaction which has been inferred to have occurred in presence of fluid (AV16b, B23a-b). To test the impact of fluid–melt immiscibility on the melt H_2O content, we added for these case studies CO_2 as a component in the system, in the amount of 1/2 and 1/4 CO_2/H_2O bulk ratio, along with the following a–x models: fluid (Connolly and Trommsdorff, 1991) and carbonates (Holland and Powell, 1998). The presence of a fluid phase has only minor effects on the H_2O content of the melt (Table S3 in the Supplement, Fig. 6). When data are pooled together, the modelled melt H_2O con-

tent is rather close (within error) to the amounts measured in re-homogenized melt inclusion (Fig. 6), e.g. the black diagonal line where the correspondence is perfect (with a 1 : 1 ratio), whereas such consideration does not hold for glassy inclusions, where the modelled H_2O content is overestimated by 2 to 4 fold (Fig. 6). Such results however suffer from the fact that modelling crustal volatiles still require more work as many issues remain (e.g. Nicoli, 2020; Carvalho et al., 2023a). For instance, uncertainties associated with the choice of starting material (e.g. Nicoli and Dyck, 2018; Palin et al., 2016) and the robustness thermodynamic models (e.g. melt) in accommodating key elements (C, Ca, Cl) (e.g. Carvalho et al., 2023a) strongly limit modelling capabilities. In addition, processes such as open system, shape of the P–T path, effective bulk composition and disequilibrium mechanisms (e.g. Evans, 2004; Villaros et al., 2009; Yakymchuk and Brown, 2014; Nicoli et al., 2017) should also be taken into consideration and could help to obtain better matches between models and nature.

5.5 Halogen in crustal melts

In this contribution we present the first NS data on Cl in preserved anatectic MI. The distribution and quantification of halogens, mainly Cl and F, in natural fluids has received considerable interest in the last decades (see Harlov and Aranovich, 2018, for an extensive review). The scientific community working on MI in magmatic rocks has devoted considerable energy to devise the best strategies to quantify these volatiles using a diverse array of in situ analytical techniques among which SIMS figures prominently (Rose-Koga et al., 2020), an effort which culminated in a comprehensive review of the approaches used to investigate MI (Esposito, 2021; Rose-Koga et al., 2021, and references therein).

At deep crustal and upper mantle levels, Cl and halogens in general are proposed to be mainly partitioned in brine (Aranovich et al., 2014). Experimental studies (Aranovich et al., 2013, 2014) have generated constraints which suggest that these fluids may influence the melting behaviour of the crust at the lower crustal to upper mantle level. As volatiles such as H_2O and halogens are redistributed into the silicate melt, high contents of Cl as well as F in silicate melts have been proposed to be possible evidence for the presence of brine during melting (Acosta-Vigil et al., 2016; Borghini et al., 2023b). Indeed, Cl has been also detected inside the nanogranitoids via EDS elemental mapping (Ferrero et al., 2012) as well as measured via EMP either on re-homogenized nanogranitoids (Borghini et al., 2023b) or in biotite crystallized from the trapped melt in MI (Axler and Ague, 2015).

Here we measured Cl via NS in OSD and GA samples and via EMP in RUB samples. GA samples show the smallest content of Cl ($\sim$ 300 ppm or 0.03 wt %). Instead, the OSD MI displays an average Cl content of 1200 ppm, with a single garnet (garnet 4 in Table 1) hosting MI with Cl $\approx$ 0.25 wt %, a value consistent with range proposed as indicative for the presence of brine during melting, from 0.2 wt % to 1.6 wt % (Ferrero et al., 2021, and references therein). Even if a brine was not present during melting of these rocks, it is possible that Cl was previously hosted in biotite, the OH phase involved in dehydration melting in these rocks based on geochemical evidence (Ferrero et al., 2019). An enrichment in Cl stabilizes biotite at T above its common stability field (Kelsey and Hand, 2015) and supports the hypothesis that these rocks underwent (delayed) biotite dehydration melting at near-UHP conditions and 875 °C (Ferrero et al., 2019). A similar explanation was also put forward to support UHT melting with biotite consumption in the CMT samples (Ferrero et al., 2021). The very dry character of the OSD metagranitoid itself may have further helped in the OSD case study, along with the high $\mathrm{d}P/\mathrm{d}T$ required to form HP felsic granulites (see discussion in Ferrero et al., 2015). In OSD samples also apatite – a common repository of Cl – is a common mineral inclusion in MI-bearing garnets, and it is also often found as trapped mineral in the nanogranitoids themselves (Ferrero et al., 2015). Coupled with the low P measured in the trapped melt when compared to the host rock (350 vs. 2500 ppm; Ferrero et al., 2018), this suggests that apatite was stable during partial melting; hence it did not contribute to the Cl melt budget.

Cl in MI from RUB samples was measured with a very focused beam (1–2 µm) due the small size of the inclusions, i.e. very far from the ideal conditions (20 µm beam diameter) suggested by Rose-Koga et al. (2021). Despite these caveats the measured Cl content, albeit low, is rather constant and it displays an average of 0.10 wt %, similar to the OSD samples. Although these melts formed at lower pressure/higher temperature with respect to the latter, both case studies display H_2O and Cl contents to have a moderate positive correlation (Fig. 3). This agrees with the experimental evidence, which suggests that H_2O and Cl have similar behaviour in silicate melts (e.g. Webster et al., 2018). As preserved glassy inclusions are generally poorer in H_2O component (see previous paragraph) with respect to the crystallized ones in the same cluster, it is likely for the actual average Cl content of the melt generated at the RUB sample locality to be actually higher.

Cl behaviour has been mostly investigated in silicic melts at low P ($\leq$ 0.1 GPa; Dolejš and Zajacz, 2018), due to its importance in ore-deposit formation, in hydrothermal systems (Lecumberri-Sanchez and Bodnar, 2018; see also LaMadrid and Steele-McInnis, 2021). Experimental results on mafic and intermediate melt seem instead to support a positive correlation between Cl and P (Webster et al., 2015), although there are still strong uncertainties due to the difficulty of constraining the dissolution behaviour of Cl in geochemically complex natural systems (Webster et al., 2018). An increase of halogen solubility with P also in silicate melts finds some support in the data from case studies of anatectic MI. Two cases studies where the melt formed at HP conditions

($P \geq 1.7$ GPa), OSD samples (this study) and CMT samples (Ferrero et al., 2021), display significant average amounts of Cl (0.12 wt % and 0.32 wt % respectively) and comparable F (0.31 wt %) for CMT only. High amounts of halogens, 0.41 wt % Cl (measured via EMP) and $\sim$0.20 wt % F (calculated), are also reported by Borghini et al. (2023b) in the nanogranitoids at Pfaffenberg in the Granulitgebirge, formed at P conditions similar to those of the OSD samples. Conversely, nanogranitoids trapped at $P < 1.3$ GPa appear to display lower average Cl contents, < 0.10 wt % (data from Gianola et al., 2021, and Acosta-Vigil et al., 2016: G21 and AVH_2O, respectively, in Table 2). Further work targeted at extending the database of Cl measurements in natural anatectic melts is however necessary to verify such correlation.

6 Concluding remarks

In this contribution we present and discuss novel NS data on both H_2O and Cl on anatectic MI and compare them to the existent database generated over a decade of NanoSIMS investigations. This allows us to draw the following considerations:

- NS appears to be the most suitable tool to investigate H_2O as well as other volatiles in objects as small as MI in metamorphic rocks.
- NS data provide hard quantitative constraints on H_2O contents of deep melts necessary to improve the existing conceptual models of crust and partial melting.
- These data support the view that the production of silicate melt in the crust, even at very high T (> 1000 °C), requires the presence of H_2O. Obviously, this does not implicitly rule out the possibility of future findings of nanogranitoids containing dry melts formed at extreme temperatures, e.g. > 1100 °C and low P.
- H_2O contents measured on some melts formed under HP conditions are remarkably close to the values expected based on melting experiments at P–T conditions close or identical to the formation of the measured melts.
- NS data just prove that anatectic MI in metamorphic rocks still contain high amounts of H_2O, up to more than 10 wt % average H_2O in one case study (Acosta-vigil et al., 2016). This provides strong evidence in support of the idea that MI can preserve their original H_2O during exhumation (Malaspina et al., 2017; see discussion in Ferrero and Angel, 2018).
- H_2O contents measured via NS appeared to be heterogeneous at the microscale since the very first NS study of nanogranitoids in metasediments. Such an occurrence was explained by the existence of a mosaic equilibrium in different microdomains undergoing melting (Bartoli et al., 2014). However, our large dataset acquired on the OSD metagranitoid shows that heterogeneities in H_2O contents, albeit less pronounced, are also visible in rocks with an igneous protolith.
- NS data on natural preserved glassy inclusions show how they cannot be regarded as directly representative of the average melt at depth in terms of H_2O content. Thus, as already proposed by Tacchetto et al. (2021), measuring the H_2O content only of natural glassy inclusions in metamorphic rocks is likely to lead to the underestimation of the melt H_2O content of $\sim$25 %–40 % with respect to the average H_2O content in the melt (this study; see also Borghini et al., 2023a).
- The investigation of halogens in anatectic MI represents a novel and fruitful research avenue to investigate the role of such consequential elements in crustal evolution (see also Borghini et al., 2023b), especially in terms of clarifying the role of brine at depth during crustal melting (e.g. Aranovich and Safonov, 2018). Our first NS data on Cl in anatectic melts, combined with H_2O data and previous work on F and Cl (Ferrero et al., 2021), show that H_2O and Cl contents in each inclusion are positively correlated, and higher P seems to favour the solubility of Cl in hot (≥ 850 °C) felsic melts.

In conclusions, NS investigation of anatectic MI is an effective approach to clarify the budget of volatiles at depth. More studies targeting these objects are thus necessary to enlarge the database and cover the wide range of lithologies which can reach melting conditions under crustal P–T–X conditions, thus helping to unravel further the intricate bundle represented by the topic of crustal differentiation and partial melting of metamorphic rocks.

Data availability. The data used in the article are included in the article (Tables 1 and 2) or in the Supplement (Tables S1–S2). Raw data can be provided by the corresponding author upon request.

Supplement. The supplement related to this article is available online at: https://doi.org/10.5194/ejm-35-1031-2023-supplement.

Author contributions. SF designed the project, collected the samples and wrote the manuscript. SF and AB conducted the study and acquired the data with the help of LR. BW performed the rehomogenization experiments with SF and AB. GN performed modelling and contributed to data interpretation. SF, AB and GN designed the art work. All authors participated in data interpretation along with RB and preparation of the manuscript.

Competing interests. At least one of the (co-)authors is a guest member of the editorial board of *European Journal of Mineralogy* for the special issue "Probing the Earth: Melt and solid inclusions as probes to understand nature". The peer-review process was guided by an independent editor, and the authors also have no other competing interests to declare.

Disclaimer. Publisher's note: Copernicus Publications remains neutral with regard to jurisdictional claims made in the text, published maps, institutional affiliations, or any other geographical representation in this paper. While Copernicus Publications makes every effort to include appropriate place names, the final responsibility lies with the authors.

Special issue statement. This article is part of the special issue "Probing the Earth: Melt and solid inclusions as probes to understand nature". It is not associated with a conference.

Acknowledgements. We thank Christine Fischer for sample preparation. We are grateful to the German Federal Ministry for Education and Research and the Deutsche Forschungsgemeinschaft (projects FE 1527/2-2, FE 1527/2-3 and FE 1527/4-1 to Silvio Ferrero). This research was supported by the Alexander von Humboldt Foundation to Gautier Nicoli. This research is part of the project no. 2021/43/P/ST10/03202 co-funded by the National Science Center and the European Union Framework Program for Research and Innovation Horizon 2020 under the Marie Skłodowska-Curie grant agreement no. 945339 to Alessia Borghini. The authors are grateful to an anonymous referee and Omar Gianola for their thoughtful and very careful reviews, which improved the clarity of the paper.

Financial support. This research has been supported by the Deutsche Forschungsgemeinschaft (grant nos. FE1527/2-2, FE1527/2-3, and FE 1527/4-1), the Alexander von Humboldt-Stiftung (Carbon in the crust), and the H2020 Marie Skłodowska-Curie Actions (grant no. 945339).

Review statement. This paper was edited by Ross Angel and reviewed by Omar Gianola and one anonymous referee.

References

Acosta-Vigil, A., London, D., Morgan VI, G. B., Cesare, B., Buick, I., Hermann, J., and Bartoli, O.: Primary crustal melt compositions: Insights into the controls, mechanisms and timing of generation from kinetics experiments and melt inclusions, Lithos, 286, 454–479, https://doi.org/10.1016/j.lithos.2017.05.020, 2007.

Acosta-Vigil, A., Buick, I., Hermann, J., Cesare, B., Rubatto, D., London, D., and Morgan VI, G. B.: Mechanisms of crustal anatexis: A geochemical study of partially melted metapelitic enclaves and host dacite, SE Spain, J. Petrol., 51, 785–821, https://doi.org/10.1093/petrology/egp095, 2010.

Acosta-Vigil, A., Buick, I., Cesare, B., London, D., and Morgan, G. B.: The extent of equilibration between melt and residuum during regional anatexis and its implications for differentiation of the continental crust: A study of partially melted metapelitic enclaves, J. Petrol., 53, 1319–1356, https://doi.org/10.1093/petrology/egs018, 2012.

Acosta-Vigil, A., Barich, A., Bartoli, O., Garrido, C. J., Cesare, B., Remusat, L., Poli, S., and Raepsaet, C.: The composition of nanogranitoids in migmatites overlying the Ronda peridotites (Betic Cordillera, S Spain): the anatectic history of a polymetamorphic basement, Contrib. Mineral. Petr., 171, 24, https://doi.org/10.1007/s00410-016-1230-3, 2016.

Acosta-Vigil, A., Cesare, B., London, D., Morgan VI, G. B.: Microstructures and composition of melt inclusions in a crustal anatectic environment, represented by metapelitic enclaves within El Hoyazo dacites, SE Spain, Chem. Geol., 235, 450–465, https://doi.org/10.1016/j.chemgeo.2006.07.014, 2017.

Aranovich, L. and Safonov, O.: Halogens in High-Grade Metamorphism, in: The Role of Halogens in Terrestrial and Extraterrestrial Geochemical Processes, Springer Geochemistry, edited by: Harlov, D. and Aranovich, L., Springer, Cham., https://doi.org/10.1007/978-3-319-61667-4_11, 2018.

Aranovich, L. Y., Newton, R. C., and Manning, C. E.: Brine-assisted anatexis: Experimental melting in the system haplogranite-H_2O-NaCl-KCl at deep-crustal conditions, Earth Planet. Sc. Lett., 374, 111–120, https://doi.org/10.1016/j.epsl.2013.05.027, 2013.

Aranovich, L. Y., Makhluf, A. R., Manning, C. E., and Newton, R. C.: Dehydration melting and the relationship between granites and granulites, Precambrian. Res., 253, 26–37, https://doi.org/10.1016/j.precamres.2014.07.004, 2014.

Axler, J. A. and Ague, J. J.: Oriented multiphase needles in garnet from ultrahigh-temperature granulites, Am. Mineral., 100, 2254–2271, https://doi.org/10.2138/am-2015-5018, 2015.

Bali, E., Hartley, M. E., Halldórsson, S. A., Gudfinnsson, G. H., and Jakobsson, S.: Melt inclusion constraints on volatile systematics and degassing history of the 2014–2015 Holuhraun eruption, Iceland, Contrib. Mineral. Petr., 173, 1–21, https://doi.org/10.1007/s00410-017-1434-1, 2018.

Barth, A. and Plank, T.: The ins and outs of water in olivine-hosted melt inclusions: hygrometer vs. speedometer, Front. Earth Sci., 9, 614004, https://doi.org/10.3389/feart.2021.614004 , 2021.

Bartoli, O.: Characterizing fluid and melt in high-grade metamorphic rocks, in: Fluid Inclusions, edited by: Lecumberri-Sanchez, P. and Steele-McInnis, M., Mineral. Assoc. Can., Short Course Ser., Vol. 49, https://doi.org/10.3749/9780921294719.ch04, 2021.

Bartoli, O. and Carvalho, B. B.: Anatectic granites in their source region: a comparison between experiments, thermodynamic modelling and nanogranitoids, Lithos, 402, 106046, https://doi.org/10.1016/j.lithos.2021.106046, 2021.

Bartoli, O., Cesare, B., Poli, S., Acosta-Vigil, A., Esposito, R., Turina, A., Bodnar, R. J., Angel, R. J., and Hunter, J.: Nanogranite inclusions in migmatitic garnet: Behavior during piston cylinder re-melting experiments, Geofluids, 13, 405–420, https://doi.org/10.1111/gfl.12038, 2013a.

Bartoli, O., Cesare, B., Poli, S., Bodnar, R. J., Acosta-Vigil, A., Frezzotti, M. L., and Meli, S.: Recovering the composition of melt and the fluid regime at the onset of crustal

anatexis and S-type granite formation, Geology, 41, 115–118, https://doi.org/10.1130/G33455.1, 2013b.

Bartoli, O., Cesare, B., Remusat, L., Acosta-Vigil, A., and Poli, S.: The H_2O content of granite embryos, Earth Planet. Sc. Lett., 395, 281–290, https://doi.org/10.1016/j.epsl.2014.03.031, 2014.

Bartoli, O., Acosta-Vigil, A., and Cesare, B.: High-temperature metamorphism and crustal melting: working with melt inclusions, Period. Mineral., 84, 3, https://doi.org/10.2451/2015PM0434, 2015.

Bartoli, O., Acosta-Vigil, A., Ferrero, S., and Cesare, B.: Granitoid magmas preserved as melt inclusions in high-grade metamorphic rocks, Am. Mineral., 101, 1543–1559, https://doi.org/10.2138/am-2016-5541CCBYNCND, 2016.

Bartoli, O., Acosta-Vigil, A., Cesare, B., Remusat, L., Gonzalez-Cano, A., Wälle, M., Tačjmanová, L., and Langone, A.: Geochemistry of Eocene-early Oligocene low-temperature crustal melts from Greater Himalayan Sequence (Nepal): a nanogranitoid perspective, Contrib. Mineral. Petr., 174, 82, https://doi.org/10.1007/s00410-019-1622-2, 2019.

Belayouni, H., Brunelli, D., Clocchiatti, R., Brunelli, D., Di Staso, A., Hassani, I. E. E. A. E., Guerrera, F., Kassaa, S., Ouazaa, N. L. M., Manuel, M. M., Serrano, F., and Tramontana, M.: La Galite Archipelago (Tunisia, North Africa): stratigraphic and petrographic revision and insights for geodynamic evolution of the Maghrebian Chain, J. Afr. Earth Sci., 56, 15–28, https://doi.org/10.1016/j.jafrearsci.2009.05.004, 2010.

Borghini, A., Ferrero, S., Wunder, B., Laurent, O., O'Brien, P. J., and Ziemann, M. A.: Granitoid melt inclusions in orogenic peridotite and the origin of garnet clinopyroxenite, Geology, 46, 1007–1010, https://doi.org/10.1130/G45316.1, 2018.

Borghini, A., Ferrero, S., Brien, P. J. O., Günter, C., Ziemann, M. A., O'Brien, P. J., Laurent, O., Günter, C., and Ziemann, M. A.: Cryptic metasomatic agent measured in situ in Variscan mantle rocks: Melt inclusions in garnet of eclogite, Granulitgebirge, Germany, J. Metamorph. Geol., 38, 207–234, https://doi.org/10.1111/jmg.12519, 2020.

Borghini, A., Nicoli, G., Ferrero, S., O'Brien, P. J., Laurent, O., Remusat, L., Borghini, G., and Milani, S.: The role of continental subduction in mantle metasomatism and carbon recycling revealed by melt inclusions in UHP eclogites, Sci. Adv., 9, eabp9482, https://doi.org/10.1126/sciadv.abp9482, 2023a.

Borghini, A., Ferrero, S., O'Brien, P. J., Wunder, B., Tollan, P., Majka, J., Fuchs, R., and Gresky, K.: Halogen-bearing metasomatizing melt preserved in high pressure (HP) eclogites of Pfaffenberg, Bohemian Massif, Eur. J. Mineral., under review, 2023b.

Brown, M.: Crustal melting and melt extraction, ascent and emplacement in orogens: mechanisms and consequences, J. Geol. Soc., 164, 709–730, https://doi.org/10.1144/0016-76492006-171, 2007.

Carvalho, B. B., Bartoli, O., Ferri, F., Cesare, B., Ferrero, S., Remusat, L., Capizzi, L. S., and Poli, S.: Anatexis and fluid regime of the deep continental crust: New clues from melt and fluid inclusions in metapelitic migmatites from Ivrea Zone (NW Italy), J. Metamorph. Geol., 37, 1–25, https://doi.org/10.1111/jmg.12463, 2018.

Carvalho, B. B., Bartoli, O., Cesare, B., Tacchetto, T., Gianola, O., Ferri, F., Aradi, L. E., and Szabó, C.: Primary CO_2-bearing fluid inclusions in granulitic garnet usually do not survive, Earth Planet. Sc. Lett., 536, 116170, https://doi.org/10.1016/j.epsl.2020.116170, 2020.

Carvalho, B. B., Bartoli, O., and Cesare, B.: C–O–H fluid-melt-rock interaction in graphitic granulites and problems of quantifying carbon budget in the lower continental crust, Chem. Geol., 631, 121503, https://doi.org/10.1016/j.chemgeo.2023.121503, 2023a.

Carvalho, B. B., Bartoli, O., Cesare, B., Satish-Kumar, M., Petrelli, M., Kawakami, T., Hokada, T., and Gilio, M.: Revealing the link between A-type granites and hottest melts from residual metasedimentary crust, Geology, 51, 845–849, https://doi.org/10.1130/G51097.1, 2023b.

Cesare, B., Salvioli Mariani, E., and Venturelli, G.: Crustal anatexis and melt extraction during deformation in the restitic xenoliths at El Joyazo (SE Spain), Mineral. Mag., 61, 15–27, https://doi.org/10.1180/minmag.1997.061.404.03, 1997.

Cesare, B., Maineri, C., Baron Toaldo, A., Pedron, D., and Acosta-Vigil, A.: Immiscibility between carbonic fluids and granitic melts during crustal anatexis: a fluid and melt inclusion study in the enclaves of the Neogene Volcanic Province of SE Spain, Chem. Geol., 237, 433–449, https://doi.org/10.1016/j.chemgeo.2006.07.013, 2007.

Cesare, B., Ferrero, S., Salvioli-Mariani, E., Pedron, D., and Cavallo, A.: Nanogranite and glassy inclusions: the anatectic melt in migmatites and granulites, Geology, 37, 627–630, https://doi.org/10.1130/G25759A.1, 2009.

Cesare, B., Acosta-Vigil, A., Bartoli, O., and Ferrero, S.: What can we learn from melt inclusions in migmatites and granulites?, Lithos, 239, 186–216, https://doi.org/10.1016/j.lithos.2015.09.028, 2015.

Clemens, J. D., Stevens, G., and Bryan, S. E.: Conditions during the formation of granitic magmas by crustal melting – Hot or cold; drenched, damp or dry?, Earth-Sci. Rev., 200, 102982, https://doi.org/10.1016/j.earscirev.2019.102982, 2020.

Condie, K. C.: Chemical composition and evolution of the upper continental crust: contrasting results from surface samples and shales, Chem. Geol., 104, 1–37, https://doi.org/10.1016/0009-2541(93)90140-E, 1993.

Connolly, J. A. D.: The geodynamic equation of state: what and how, Geochem. Geophy. Geosy., 10, Q10014, https://doi.org/10.1029/2009GC002540, 2010.

Connolly, J. A. D. and Thompson, A. B.: Fluid and enthalpy production during regional metamorphism, Contrib. Mineral. Petr., 102, 347–366, https://doi.org/10.1007/BF00373728, 1989.

Connolly, J. A. D. and Trommsdorff, V.: Petrogenetic grids for metacarbonate rocks: pressure-temperature phase-diagram projection for mixed-volatile systems, Contrib. Mineral. Petr., 108, 93–105, https://doi.org/10.1007/BF00307329, 1991.

Créon, L., Levresse, G., Remusat, L., Bureau, H., and Carrasco-Núñez, G.: New method for initial composition determination of crystallized silicate melt inclusions, Chem. Geol., 483, 162–173, https://doi.org/10.1016/j.chemgeo.2018.02.038, 2018.

Diener, J. F. A. and Powell, R.: Revised activity–composition models for clinopyroxene and amphibole, J. Metamorph. Geol., 30, 131–142, https://doi.org/10.1111/j.1525-1314.2011.00959.x, 2012.

Dolejš, D. and Zajacz, Z.: Halogens in Silicic Magmas and Their Hydrothermal Systems, in: The Role of Halogens in Terrestrial and Extraterrestrial Geochemical Processes, edited by: Harlov,

D. and Aranovich, L., Springer Geochemistry, Springer, Cham., https://doi.org/10.1007/978-3-319-61667-4_7, 2018.

Esposito, R.: A protocol and review of methods to select, analyze and interpret melt inclusions to determine pre-eruptive volatile contents of magmas, in: Fluid Inclusions, edited by: Lecumberri-Sanchez, P. and Steele-McInnis, M., Mineral. Assoc. Can., Short Course Ser., 49, 163–194, https://doi.org/10.3749/9780921294719.ch07, 2021.

Esposito, R., Hunter, J., Schiffbauer, J. D., and Bodnar, R. J.: An assessment of the reliability of melt inclusions as recorders of the pre-eruptive volatile content of magmas, Am. Mineral., 99, 976–998, https://doi.org/10.2138/am.2014.4574, 2014.

Esposito, R., Redi, D., Danyushevsky, L. V., Gurenko, A., De Vivo, B., Manning, C. E., Bodnar, R. J., Steele-MacInnis, M., and Frezzotti, M.-L.: Constraining the volatile evolution of mafic melts at Mt. Somma–Vesuvius, Italy, based on the composition of reheated melt inclusions and their olivine hosts, Eur. J. Mineral., 35, 921–948, https://doi.org/10.5194/ejm-35-921-2023, 2023.

Evans, T. P.: A method for calculating effective bulk composition modification due to crystal fractionation in garnet-bearing schist: Implications for isopleth thermobarometry, J. Metamorph. Geol., 22, 547–557, https://doi.org/10.1111/j.1525-1314.2004.00532.x, 2004.

Ferrero, S. and Angel, R. J.: Micropetrology: Are inclusions grains of truth?, J. Petrol., 59, 1671–1700, https://doi.org/10.1093/petrology/egy075, 2018.

Ferrero, S., Bartoli, O., Cesare, B., Salvioli-Mariani, E., Acosta-Vigil, A., Cavallo, A., Groppo, C., and Battiston, S.: Microstructures of melt inclusions in anatectic metasedimentary rocks, J. Metamorph. Geol., 30, 303–322, https://doi.org/10.1111/j.1525-1314.2011.00968.x, 2012.

Ferrero, S., Braga, R., Berkesi, M., Cesare, B., and Laridhi Ouazaa, N.: Production of metaluminous melt during fluid-present anatexis: an example from the Maghrebian basement, La Galite Archipelago, central Mediterranean, J. Metamorph. Geol., 32, 209–225, https://doi.org/10.1111/jmg.12068, 2014.

Ferrero, S., Wunder, B., Walczak, K., Ziemann, M. A., and O'Brien, P. J.: Preserved near ultrahigh-pressure melt from continental crust subducted to mantle depths, Geology, 43, 447–450, https://doi.org/10.1130/G36534.1, 2015.

Ferrero, S., Ziemann, M. A., Angel, R. J., O'Brien, P. J., and Wunder, B.: Kumdykolite, kokchetavite, and cristobalite crystallized in nanogranites from felsic granulites, Orlica-Snieznik Dome (Bohemian Massif): not an evidence for ultrahigh-pressure conditions, Contrib. Mineral. Petr., 171, 1–12, https://doi.org/10.1007/s00410-015-1220-x, 2016.

Ferrero, S., O'Brien, P. J., Borghini, A., Wunder, B., Wälle, M., Günter, C., and Ziemann, M. A.: A treasure chest full of nanogranitoids: an archive to investigate crustal melting in the Bohemian Massif, in Metamorphic Geology: Microscale to Mountain Belts, Geol. Soc. Lond. Spec. Publ., 478, 13–38, https://doi.org/10.1144/SP478.19, 2019.

Ferrero, S., Ague, J. J., O'Brien, P. J., Wunder, B., Remusat, L., Ziemann, M. A., and Axler, J.: High pressure, halogen-bearing melt preserved in ultra-high temperature felsic granulites of the Central Maine terrane, Connecticut (US), Am. Mineral., 106, 1225–1236, https://doi.org/10.2138/am-2021-7690, 2021.

Ferri, F., Cesare, B., Bartoli, O., Ferrero, S., Palmeri, R., Remusat, L., and Poli, S.: Melt inclusions at MT. Edixon (Antarctica): Chemistry, petrology and implications for the evolution of the Lanterman range, Lithos, 374–375, 105685, https://doi.org/10.1016/j.lithos.2020.105685, 2020.

Frezzotti, M. L. and Ferrando, S.: The chemical behavior of fluids released during deep subduction based on fluid inclusions, Am. Mineral., 100, 352–377, https://doi.org/10.2138/am-2015-4933, 2015.

Gianola, O., Bartoli, O., Ferri, F., Galli, A., Ferrero, S., Capizzi, L. S., Liebske, C., Remusat, L., Poli, S., and Cesare, B.: Anatectic melt inclusions in ultra-high temperature granulites, J. Metamorph. Geol., 39, 321–342, https://doi.org/10.1111/jmg.12567, 2021.

Hagen, B., Hoernes, S., and Rötzler, J.: Geothermometry of the ultrahigh-temperature Saxon granulites revisited. Part II: Thermal peak conditions and cooling rates inferred from oxygen-isotope fractionations, Eur. J. Mineral., 20, 1117–1133, https://doi.org/10.1127/0935-1221/2008/0020-1858, 2008.

Harlov, D. E. and Aranovich, L.: The Role of Halogens in Terrestrial and Extraterrestrial Geochemical Processes: Surface, Crust, and Mantle, in: The Role of Halogens in Terrestrial and Extraterrestrial Geochemical Processes, edited by: Harlov, D. and Aranovich, L., Springer Geochemistry, Springer, Cham., https://doi.org/10.1007/978-3-319-61667-4_1, 2018.

Hauri, E.: SIMS analysis of volatiles in silicate glasses, 2: isotopes and abundances in Hawaiian melt inclusions, Chem. Geol., 183, 115–141, 2002.

Hermann, J. and Rubatto, D.: Subduction of continental crust to mantle depth: geochemistry of ultrahigh-pressure rocks, in: Treatise on Geochemistry, edited by: Holland, H. D. and Turekian, K. K., 2nd Edn., Oxford, Elsevier, 309–340, https://doi.org/10.1016/B978-0-08-095975-7.00309-0, 2014.

Hermann, J. and Spandler, C. J.: Sediment melts at sub-arc depths: an experimental study, J. Petrol., 49, 717–740, https://doi.org/10.1093/petrology/egm073, 2008.

Holland, T. and Powell, R.: Activity–composition relations for phases in petrological calculations: an asymmetric multicomponent formulation, Contrib. Mineral. Petr., 145, 492–501, https://doi.org/10.1007/s00410-003-0464-z, 2003.

Holland, T. J. B. and Powell, R. T. J. B.: An internally consistent thermodynamic data set for phases of petrological interest, J. Metamorph. Geol., 16, 309–343, https://doi.org/10.1111/j.1525-1314.1998.00140.x, 1998.

Humphreys, M. C., Kearns, S. L., and Blundy, J. D.: SIMS investigation of electron-beam damage to hydrous, rhyolitic glasses: Implications for melt inclusion analysis, Am. Mineral., 91, 667–679, https://doi.org/10.2138/am.2006.1936, 2006.

Johannes, W. and Holtz, F.: Petrogenesis and experimental petrology of granitic rocks, 335 pp., Berlin, Springer, 1996.

Kelsey, D. E. and Hand, M.: On ultrahigh temperature crustal metamorphism: Phase equilibria, trace element thermometry, bulk composition, heat sources, timescales and tectonic settings, Geosci. Front., 6, 311–356, https://doi.org/10.1016/j.gsf.2014.09.006, 2015.

Lamadrid, H. M. and Steele-McInnis, M.: Crustal melting: Deep, hot, and salty, Am. Mineral., 106, 1193–1194, https://doi.org/10.2138/am-2022-8108, 2021.

Lecumberri-Sanchez, P. and Bodnar, R. J.: Halogen Geochemistry of Ore Deposits: Contributions Towards Understanding Sources and Processes, in: The Role of Halogens in Terrestrial

and Extraterrestrial Geochemical Processes, edited by: Harlov, D. and Aranovich, L., Springer Geochemistry, Springer, Cham., https://doi.org/10.1007/978-3-319-61667-4_5, 2018.

Liu, Q., Liu, P., Li, X., and Zhang, J.: The origin and compositions of melt inclusions in an Al_2SiO_5-free paragneiss from the Namche Barwa Complex in the Eastern Himalayan Syntaxis, J. Metamorph. Geol., 41, 879–898, https://doi.org/10.1111/jmg.12721, 2023.

Lowenstern, J. B.: Applications of silicate-melt inclusions to the study of magmatic volatiles, in: Magmas, Fluids and Ore Deposits, edited by: Thompson, J. F. H., Short Course Handbook, Mineralogical Society of Canada, Nepean, Ont., 23, 71–99, 1995.

Makhluf, A. R., Newton, R. C., and Manning, C. E.: Experimental determination of liquidus H_2O contents of haplogranite at deep-crustal conditions, Contrib. Mineral. Petr., 172, 77, https://doi.org/10.1007/s00410-017-1392-7, 2017.

Malaspina, N., Langenhorst, F., Tumiati, S., Campione, M., Frezzotti, M. L., and Poli, S.: The redox budget of crust-derived fluid phases at the slab–mantle interface, Geochim. Cosmochim. Ac., 209, 70–84, https://doi.org/10.1016/j.gca.2017.04.004, 2017.

Metrich, N. and Wallace, P. J.: Volatile abundances in basaltic magmas and their degassing paths tracked by melt inclusions, in: Minerals, Inclusions and Volcanic Processes, edited by: Putirka, K. D. and Tepley III, F. J., Mineral. Soc. Amer. Geochem. Soc., Rev. Mineral. Geochem., 69, 363–402, https://doi.org/10.2138/rmg.2008.69.10, 2008.

Mirwald, P. W. and Massonne, H.-J.: Quartz-coesite transition and the comparative friction measurements in piston-cylinder apparatus using talc-alsimag glass (TAG) and NaCl high pressure cells: A discussion, Neues Jb. Miner., 10, 469–477, 1980.

Morgan, G. B. and London, D.: Effect of current density on the electron microprobe analysis of alkali aluminosilicate glasses, Am. Mineral., 90, 1131–1138, https://doi.org/10.2138/am.2005.1769, 2005.

Nicoli, G.: Water budget and partial melting in an Archean crustal column: example from the Dharwar Craton, India, Geol. Soc. Lond. Spec. Publ., 489, 115–133, https://doi.org/10.1144/SP489-2018-88, 2020.

Nicoli, G. and Dyck, B.: Exploring the metamorphic consequences of secular change in the siliciclastic compositions of continental margins, Geosci. Front., 9, 967–975, https://doi.org/10.1016/j.gsf.2017.12.009, 2018.

Nicoli, G. and Ferrero, S.: Nanorocks, volatiles and plate tectonics, Geosci. Front., 12, 101188, https://doi.org/10.1016/j.gsf.2021.101188, 2021.

Nicoli, G., Stevens, G., Moyen, J. F., Vezinet, A., and Mayne, M.: Insights into the complexity of crustal differentiation: K_2O-poor leucosomes within metasedimentary migmatites from the Southern Marginal Zone of the Limpopo Belt, South Africa, J. Metamorph. Geol., 35, 999–1022, 2017.

Nicoli, G., Borghini, A., and Ferrero, S.: The carbon budget of crustal reworking during continental collision: clues from nanorocks and fluid inclusions, Chem. Geol., 608, 121025, https://doi.org/10.1016/j.chemgeo.2022.121025, 2022a.

Nicoli, G., Gresky, K., and Ferrero, S.: Mesoarchean melt and fluid inclusions in garnet from the Kangerlussuaq basement, Southeast Greenland, Mineralogia, 53, 1–9, https://doi.org/10.2478/mipo-2022-0001, 2022b.

Palin, R. M., White, R. W., Green, E. C., Diener, J. F., Powell, R., and Holland, T. J.: High-grade metamorphism and partial melting of basic and intermediate rocks, J. Metamorph. Geol., 34, 871–892, https://doi.org/10.1111/jmg.12212, 2016.

Roberts, M. P. and Finger, F.: Do U–Pb zircon ages from granulites reflect peak metamorphic conditions?, Geology, 25, 319–322, https://doi.org/10.1130/0091-7613(1997)025<0319:DUPZAF>2.3.CO;2, 1997.

Roedder, E.: Origin and significance of magmatic inclusions, B. Minéral., 102, 5–6, https://doi.org/10.3406/bulmi.1979.7299, 1979.

Roedder, E.: Fluid Inclusions, Mineralogical Society of America, 12, 644 pp., 1984.

Rose-Koga, E. F., Koga, K. T., Devidal, J.-L., Shimizu, N., Le Voyer, M., Dalou, C., and Doebeli, M.: In-situ measurements of magmatic volatile elements, F, S and Cl by electron microprobe, secondary ion mass spectrometry, and elastic recoil detection analysis, Am. Mineral., 105, 616–626, https://doi.org/10.2138/am-2020-7221, 2020.

Rose-Koga, E. F., Bouvier, A.-S., Gaetani, G. A., Wallace, P. J., Allison, C. M., Andrys, J. A., Angeles de la Torre, C. A., Barth, A., Bodnar, R. J., Bracco Gartner, A. J. J., Butters, D., Castillejo, A., Chilson-Parks, B., Choudhary, B. R., Cluzel, N., Cole, M., Cottrell, E., Daly, A., Danyushevsky, L. V., DeVitre, C. L., Drignon, M. J., France, L., Gaborieau, M., Garcia, M. O., Gatti, E., Genske, F. S., Hartley, M. E., Hughes, E. C., Iveson, A. A., Johnson, E. R., Jones, M., Kagoshima, T., Katzir, Y., Kawaguchi, M., Kawamoto, T., Kelley, K. A., Koornneef, J. M., Kurz, M. D., Laubier, M., Layne, G. D., Lerner, A., Lin, K.-Y., Liu, P.-P., Lorenzo-Merino, A., Luciani, N., Magalhães, N., Marschall, H. R., Michael, P. J., Monteleone, B. D., Moore, L. R., Moussallam, Y., Muth, M., Myers, M. L., Narváez, D. F., Navon, O., Newcombe, M. E., Nichols, A. R. L., Nielsen, R. L., Pamukcu, A., Plank, T., Rasmussen, D. J., Roberge, J., Schiavi, F., Schwartz, D., Shimizu, K., Shimizu, K., Shimizu, N., Thomas, J. B., Thompson, G. T., Tucker, J. M., Ustunisik, G., Waelkens, C., Zhang, Y., and Zhou, T.: Silicate melt inclusions in the new millennium: A review of recommended practices for preparation, analysis, and data presentation, Chem. Geol., 570, 120145, https://doi.org/10.1016/j.chemgeo.2021.120145, 2021.

Rosenberg, C. L. and Handy, M. R.: Experimental deformation of partially melted granite revisited: implications for the continental crust, J. Metamorph. Geol., 23, 19–28, https://doi.org/10.1111/j.1525-1314.2005.00555.x, 2005.

Rötzler, J., Hagen, B., and Hoernes, S.: Geothermometry of the ultrahigh-temperature Saxon granulites revisited. Part I: New evidence from key mineral assemblages and reaction textures, Eur. J. Mineral., 20, 1097–1115, https://doi.org/10.1127/0935-1221/2008/0020-1857, 2008.

Scaillet, B., Holtz, F., Pichavant, M., and Schmidt, M.: Viscosity of Himalayan leucogranites: implications for mechanisms of granitic magma ascent, J. Geophys. Res., 101, 27691–27699, https://doi.org/10.1029/96JB01631, 1996.

Sobolev, A. V.: Melt inclusions in minerals as a source of principal petrological information, Petrology, 4, 209–220, 1996.

Sorby, H. C.: On the microscopical structure of crystals, indicating the origin of minerals and rocks, Q. J. Geol. Soc. Lond., 14, 453–500, 1858.

Tacchetto, T., Reddy, S. M., Bartoli, O., Rickard, D. A., Fougerouse, D., Saxey, D. W., Quadir, Z., and Clark, C.: Pre-nucleation geochemical heterogeneity within glassy anatectic inclusions and the role of water in glass preservation, Contrib. Mineral. Petr., 176, 70, https://doi.org/10.1007/s00410-021-01826-0, 2021.

Thomen, A., Robert, F., and Remusat, L.: Determination of the nitrogen abundance in organic materials by NanoSIMS quantitative imaging, J. Anal. Atom. Spectrom., 29, 512–519, 2014.

Villaros, A., Stevens, G., Moyen, J. F., and Buick, I. S.: The trace element compositions of S-type granites: evidence for disequilibrium melting and accessory phase entrainment in the source, Contrib. Mineral. Petr., 158, 543–561, https://doi.org/10.1007/s00410-009-0396-3, 2009.

Wannhoff, I., Ferrero, S., Borghini, A., Darling, R., and O'Brien, P. J.: First evidence of dmisteinbergite (CaAl2Si2O8 polymorph) in high grade metamorphic rocks, Am. Mineral., 107, 2315–2319, https://doi.org/10.2138/am-2022-8505, 2022.

Webster, J. D., Vetere, F., Botcharnikov, R. E., Goldoff, B., McBirney, A., Doherty, A. L.: Experimental and modeled chlorine solubilities in aluminosilicate melts at 1 to 7000 bars and 700 to 1250 °C: Applications to magmas of Augustine Volcano, Alaska, Am. Mineral., 100, 522–535, https://doi.org/10.2138/am-2015-5014, 2015.

Webster, J. D., Baker, D. R., and Aiuppa, A.: Halogens in Mafic and Intermediate-Silica Content Magmas, in: The Role of Halogens in Terrestrial and Extraterrestrial Geochemical Processes, edited by: Harlov, D. and Aranovich, L., Springer Geochemistry, Springer, Cham., https://doi.org/10.1007/978-3-319-61667-4_6, 2018.

Weinberg, R. F. and Hasalová, P.: Water-fluxed melting of the continental crust: A review, Lithos, 212–215, 158–188, https://doi.org/10.1016/j.lithos.2014.08.021, 2015.

White, R. W., Powell, R., Holland, T. J. B., and Worley, B. A.: The effect of TiO_2 and Fe_2O_3 on metapelitic assemblages at greenschist and amphibolite facies conditions: mineral equilibria calculations in the system K_2O-FeO-MgO-Al_2O_3-SiO_2-H_2O-TiO_2-Fe_2O_3, J. Metamorph. Geol., 18, 497–512, https://doi.org/10.1046/j.1525-1314.2000.00269.x, 2000.

White, R. W., Powell, R., and Johnson, T. E.: The effect of Mn on mineral stability in metapelites revisited: New a–x relations for manganese-bearing minerals, J. Metamorph. Geol., 32, 809–828, https://doi.org/10.1111/jmg.12095, 2014.

Whitney, D. L. and Evans, B. W.: Abbreviations for names of rock-forming minerals, Am. Mineral., 95, 185–187, https://doi.org/10.2138/am.2010.3371, 2010.

Wickham, S. M.: The segregation and emplacement of granitic magmas, J. Geol. Soc., 144, 281–297, https://doi.org/10.1144/gsjgs.144.2.0281, 1987.

Yakymchuk, C. and Brown, M.: Consequences of open-system melting in tectonics, J. Geol. Soc., 171, 21–40, https://doi.org/10.1144/jgs2013-039, 2014.

Yardley, B. W. D.: The role of water in the evolution of the continental crust, J. Geol. Soc., 166, 585–600, https://doi.org/10.1144/0016-76492008-101, 2009.